Hyloidichnus trackways with digit and tail drag traces from the Permian of Gonfaron (Var, France): new insights on the locomotion of captorhinomorph eureptiles

A. Logghe[1*], E. Mujal[2,3], L. Marchetti[4], A. Nel[5], J.-M. Pouillon[6], S. Giner[7], R. Garrouste[5], J.-S. Steyer[1].

[1]Centre de Recherches en Paléontologie de Paris, UMR 7202 – CNRS, MNHN, SU, EPHE, Muséum National d'Histoire Naturelle, Sorbonne Universités, 8 rue Buffon, CP38, F-75005 Paris, France.

[2]Staatliches Museum für Naturkunde Stuttgart, Rosenstein 1, D-70191 Stuttgart, Germany.

[3]Institut Català de Paleontologica M. Crusafont, ICTA-ICP building, c/ de les columnes, s/n, E-08193 Cerdanyola del Vallès, Catalonia, Spain.

[4]Museum für Naturkunde Berlin, Leibniz-Institut für Evolutions- und Biodiversitätsforschung, Invalidenstrasse 43, 10115 Berlin, Germany.

[5]Institut de Systématique, Evolution, Biodiversité, ISYEB – UMR 7205 – CNRS, MNHN, SU EPHE, Muséum National d'Histoire Naturelle, Sorbonne Universités, Université des Antilles, 57 rue Cuvier, CP 50, Entomologie, F-75005, Paris, France.

[6]Nivolas Vermelle, France.

[7]Service d'Archéologie, Direction de l'Ingénierie Territoriale, Département du Var, 57 rue Gustave Bret, Fréjus, France.

Antoine Logghe: antoine.logghe@edu.mnhn.fr (corresponding author)

https://orcid.org/0000-0002-2854-77

Eudald Mujal: eudald.mujalgrane@smns-bw.de

https://orcid.org/0000-0002-6310-323X

Lorenzo Marchetti: lorenzo.marchetti85@gmail.com

https://orcid.org/0000-0002-1047-7887

André Nel: andre.nel@mnhn.fr

https://orcid.org/0000-0002-4241-7651

Jean-Marc Pouillon: jmpdb@wanadoo.fr

https://orcid.org/0000-0001-6016-4734

Stephen Giner: sginer@var.fr

Romain Garrouste: romain.garrouste@mnhn.fr

https://orcid.org/0000-0002-0880-5781

Jean-Sébastien Steyer: jean-sebastien.steyer@mnhn.fr

https://orcid.org/0000-0003-1835-7852

Abstract – Newly discovered tetrapod footprints from the middle Permian Pelitic Formation of Gonfaron (Le Luc Basin, Var, France) are described in detail and assigned to the ichnogenus *Hyloidichnus*. These specimens are very well-preserved, with detailed trackways showing anatomical features, digit drag traces and continuous tail impressions. Together with other *Hyloidichnus* specimens from the same locality and from the University of Burgundy collections, they allow the identification of the possible trackmakers of *Hyloidichnus*: small *Hyloidichnus* footprints are correlated with captorhinomorphs with autopodia similar to *Captorhinus* whereas large *Hyloidichnus* footprints might be correlated with larger captorhinomorphs or other 'basal' (eventually stem-) moradisaurines. A detailed comparative analysis is proposed to better understand the locomotion style of the trackmakers. Starting from the reconstruction of the stance phase of *Captorhinus*, we document the swing phase of the fore- and hind-limbs of captorhinomorphs thanks to the continuous digit drag traces associated

with *Hyloidichnus*. A link between gait and track preservation have been highlighted through the analysis of tail impressions and high-resolution 3D models. In all, this study increases our understanding of captorhinomorph locomotion and enhances the integration of both tracks and skeletal remains to highlight the biomechanics of Permian tetrapods.

Keywords – Biomechanics, Guadalupian-Wordian, tetrapod footprints, track-trackmaker correlation, *Catporhinus*, ichnology.

1. Introduction

Fossil footprints provide qualitative and quantitative information on anatomy and behaviour of ancient tetrapods. This includes valuable data on, for example, functional morphology and locomotion of the trackmakers (Voigt et al., 2007; Romano et al., 2016; Marchetti et al, 2017; Buchwitz and Voigt, 2018; Mujal and Marchetti, 2020; Mujal and Schoch, 2020; Mujal et al., 2020). Tetrapod footprints are usually compared with the morphology of the appendicular skeletons of contemporary taxa (Gand, 1987; Voigt, 2005; Gand and Durand, 2006; Voigt et al., 2007; Marchetti et al., 2019a, 2020a; Mujal and Marchetti, 2020; Mujal and Schoch, 2020). To render these studies possible, well-preserved tracks and trackways are needed: these exhibit morphological features directly related to anatomy, without 'extramorphologies' (i.e., morphological features that hide anatomical traits of the producer; Peabody, 1948; Haubold et al., 1995; Marchetti et al., 2019b). Tetrapod footprints arranged in pes-manus couples along trackways provide important information on the trunk length and pes and manus orientation of the trackmaker. Moreover, the possible presence of a continuous tail impression as well as digit drag traces can be key elements to perform a locomotion reconstruction (e.g., Bernardi and Avanzini, 2011; Marchetti et al., 2017; Mujal et al., 2017).

One of the most important amniote clades of the Palaeozoic is the Captorhinomorpha (and closely-related protorothyridids). Captorhinomorph eureptiles are relatively well-known thanks to various body fossils from the Permian of Europe, America and Africa, but their footprints were less-intensively studied, although common (e.g., Voigt and Lucas, 2018). Consequently, studies that correlate Captorhinomorpha track and skeletal records are rare (e.g., Voigt et al., 2010; Marchetti et al., 2020b). Palaeozoic footprints attributable to this group are probably represented by three ichnogenera: *Hyloidichnus* Gilmore, 1927, *Merifontichnus* Gand et al., 2000 and *Notalacerta* Butts, 1891 (e.g., Marchetti et al., 2020b). Although *Hyloidichnus* is generally attributed to captorhinomorphs (e.g., Voigt et al., 2010), precise studies correlating tracks and trackmakers and analysing locomotion patterns are lacking. Here, we describe in detail four *Hyloidichnus* trackways from the Permian Pelitic Formation of Gonfaron (Le Luc Basin, Provence, France). This material is exceptionally well-preserved, with continuous tail and digit drag traces, and allows a confident correlation of *Hyloidichnus* with captorhinomorph eureptiles with autopodia similar to *Captorhinus* and the performance of a precise analysis of the trackmaker step cycle. This brings new insights on the locomotion of Permian tetrapods and adds new elements on the possible disparities amongst different clades (Mujal et al., 2020).

2. Geological setting

The Permian basins of Provence are from East to West (Fig. 1A) the Estérel and Bas-Argens basins bordered to the north by the Tanneron massif, and the Luc and Toulon-Cuers basins bordered to the South by the Maures massif and the Mediterranean Sea. The Luc and Toulon-Cuers basins are bounded to the North by a thin deposit of Triassic non-marine sediments ('Buntsandstein', Anisian) followed by thick deposits of Mesozoic sediments (see Fig. 1A) (Durand et al., 2011). The topography of these basins is strongly marked by the

Permian depression that extends from the Toulon-Cuers Basin to the Bas-Argens Basin, corresponding to the erosion of the sedimentary fill of the Toulon-Cuers and Le Luc basins.

The Pelitic Formation is the upper formation of the Luc Basin. It is dated to the Guadalupian, possibly Wordian, according to radioisotopic ages, palaeomagnetism and correlation of the underlying units with fossil-bearing units of nearby basins, which include macrofloral remains, sporomorphs, ostracods, insects and tetrapod footprints (Gand and Durand, 2006; Durand, 2008; Garrouste et al., 2017). The material has been found within a red pelitic level of about 3 m thick that ends with a layer of indurated argilits in laminated plates containing mudcracks, ripple marks and raindrops. This red pelitic level also yields abundant ichnites on bio-mats, arthropod trace fossils (*Scoyenia*, *Planolites* and *Acripes multiformis*) and arthropod trackways (*Lithographus hieroglyphus*), and cone ichnofossils. Several tetrapod trackways such as *Hyloidichnus major*, *Hyloidichnus* isp, *Microsauripus/Varanopus* isp., *Dromopus* isp. and *Batrachichnus salamandroides* have also been recovered. This ichno-assemblage characterises a facies close to exondation and a possible ephemeral lake of decametric extension, attracting an abundant fauna.

3. Material and methods

Abbreviations: GONF-A: Gonfaron collection of the MNHN; GONF-G: Gonfaron collection of the University of Burgundy collected by G. Gand.

The four trackways described here have been found on the same locality, the ‘Gonfaron A site’ near the eponymous village, Var Département, Southern France. They come from the middle Permian Pelitic Formation of the Le Luc Basin, Provence (Fig. 1). Among the four specimens analysed here, two (GONF-A-04 and GONF-A-11) have been recently discovered by one of us (RG; GPS coordinates available on request from corresponding author) and are stored at the Muséum National d’Histoire Naturelle, Paris (France) (MNHN). The two others,

from the University of Burgundy (Dijon, France) collections (GONF-G20 and GONF-G21), were previously described by Gand (1987, 1989):

- GONF-A-04 (Fig. 2) is a slab of 266 x 200 mm with a trackway consisting of four consecutive pes-manus couples (Nr. 1-4 Fig. 2), a tail impression (Nr. 5 Fig. 2) and digit drag traces (Nr. 6 and 6' Fig. 2), preserved in concave epirelief.

- GONF-A-11 (Fig. 3) is a slab of 298 × 331 mm with a partial trackway consisting of two pes-manus couples, a right manus and a continuous tail impression, preserved in concave epirelief.

- GONF-G20 (Fig. 4) is a slab of 479 × 364 mm and corresponds to a part (GONF-G20A, in concave epirelief) and its partial counterpart (GONF-G20B, in convex hyporelief). It preserves tracks of two ichnotaxa, an incomplete step cycle of *Hyloidichnus* (see description below) and the holotype of *Varanopus rigidus*. The step cycle of *Hyloidichnus* includes a right manus, a right pes-manus couple, a left pes-manus couple and continuous digit drag traces.

- GONF-G21A (Fig. 5) is a slab of 463 mm × 227 mm and includes a trackway consisting of six consecutive pes-manus couples, continuous digit drag traces and a continuous tail impression, artificial gypsum cast in convex hyporelief. GONF-G21B is a partial counterpart of the original, from which GONF-G21A was casted, preserved in convex hyporelief.

The specimens were examined with oblique light and photographed with a Nikon D800 and a Canon EOS 70D and then digitally drawn using Krita v.4.2.9 and Adobe Illustrator CC 2020. Quantitative and qualitative analyses were carried out following the protocols of Haubold (1971), Leonardi (1987) and Gand (1987) for tetrapod footprints and Hasiotis et al. (2007) for tetrapod tail impressions. Measurements were taken using ImageJ2. 3D models were obtained through scans and photogrammetry. Scans were done with a triangulation-based laser scanner

(Next Engine 3D Scanner®). Close-range photogrammetry was performed using photos taken with a Nikon D800 (60 mm macro lens) and a Canon EOS 70D and the software Agisoft Photoscan (standard version 1.1.4) and Meshlab 2020.03 for 3D model generation and edition. Paraview v. 5.8.0 was used for the generation of colour-coded height maps and contours (e.g., Falkingham, 2012; Mujal et al., 2016, 2020). The track-trackmaker correlation was performed using an anatomy-based correlation (e.g., Voigt et al., 2007; Marchetti et al., 2017, 2019a; Mujal and Marchetti, 2020) between the best-preserved tracks and the manus and pes skeletons of *Captorhinus* described by Holmes (1977, 2003), including a comparison with other possible producers. The track preservation was evaluated by means of morphological preservation *sensu* Marchetti et al. (2019b). The measurements of the manus and pes parameters were done on the reconstructions provided by Holmes (1977, fig. 11; 2003, fig. 7). The ratio including the body length was calculated with measurements on the *Captorhinus aguti* skeleton from the Field Museum of Chicago, specimen FMC-UC 491, Clear Fork Group (Kungurian), Texas.

4. Systematic palaeontology

Hyloidichnus Gilmore, 1927

Hyloidichnus isp.

Figs. 2-5, Tables 1-4

Referred specimens: GONF-A-04; GONF-A-11; GONF-G20; GONF-G21.

Description: The manus footprints are semi-plantigrade, the pes footprints are semi-plantigrade to semi-digitigrade. Both manus and pes tracks show a medial-lateral decrease in relief, although this feature is more distinct in the pes. The manus tracks are wider (22 to 76 mm) than long (19.2 to 64 mm). The pes tracks are larger than the manus tracks and almost as long (28 to 61 mm) as wide (25 to 75 mm).

Manus and pes tracks are pentadactyl and ectaxonic (digit IV imprint is the longest). The relative lengths of the manus digit impressions are I<V≤II<III<IV, the relative lengths of the pes digit impressions are I<V<II<III<IV. The divarication angle of the digits I-V imprints of the manus is around 140°. The divarication angle of the digits I-V of the pes is around 170°. The digit impressions are straight, relatively thin and long. The imprints of digits I and IV are slightly directed inwards, whereas the digit V impressions are often directed outwards. The digits of both manus and pedes were clawed, as indicated by the T-shaped tip impressions (digit tip bifurcation) in most of specimens; otherwise, in GONF-A-04 some pes tracks end in thin tip impressions. In GONF-A-04, expulsion rims associated with both manus and pes tracks are higher around the impressions of digits I, II and III. They are clearer in association with the digit impressions of the manus, where they seem to follow precisely the shape of the digit.

The palm impressions are slightly wider (15 to 30.5 mm) than long (12 to 33 mm), whereas the sole impressions are much wider (16 to 22.5 mm) than long (7 to 13 mm). The palm and sole impressions are shallower just beneath the digit IV and V impressions, and the proximal margin of the palm/sole can be slightly convex proximally or rectilinear.

The manus tracks are placed in front of the pes, at distances between 19 to 39 mm. The manus tracks are closer to and rotated towards the trackway midline, the pes imprints are almost parallel to or slightly rotated outwards (even though some pes tracks show an inward rotation) relative to the trackway midline. The pace angulations are greater than 90° in the manus tracks and slightly lower than 90° in the pes tracks. The pes imprints are distanced about 10 mm from the tail impression (Nr. 5 in Fig. 2). The tail impression observed in GONF-A-04 is 156 mm long and 5.5 mm wide (maximum value) and is mainly straight, with a low sinusoidal (2.7 mm) shape and a high wavelength (90 mm). A regular pattern is observed with a widening of the tail impression in proximity of the pes-manus couples. In GONF-G21 (Fig. 5), the tail impression is straight (sinuosity of ~1 mm) without identifiable wavelength, whereas in GONF-A-11 (Fig.

3) it has a high sinuosity with an amplitude of about 52 mm and a wavelength of 123.5 mm. It also shows a 1 mm deep furrow at its midline.

In GONF-A-04, digit drag traces characterised by four curved thin grooves are preserved from the pes of couple Nr. 1 to the pes of couple Nr. 2 (Fig. 2). These impressions are associated with pedal digits II, III, IV and V. Three similar grooves corresponding to digit drag traces are proximal to the pes of couple Nr. 1 (Fig. 2): they are probably departing from the previous pes-manus couple (not preserved on the slab). The digit drag traces do not start directly from the digits and seem to be partially stepped over by the pes and the manus tracks. A second similar trace with three grooves departing from the pes of the couple Nr. 2 (Fig. 2) is also visible but poorly preserved. In GONF-G20 (Fig. 4), three to four digit drag traces are also preserved from one pes to another and associated with the digits II to V. In GONF-G21 (Fig. 5), three to four digit drag traces are preserved, either from the pes to the following pes of the next pes-manus couple and associated with digits II to V or three digit drag traces from the manus to the following manus of the next pes-manus couple and associated with digits III to V. The digit drag traces of these two specimens are larger than those on GONF-A-04.

Remarks: The straight digit imprints with clawed to bifurcated tip impressions in both pes and manus tracks, the relative length of the digit impressions, increasing from I to IV, with digits III and IV of similar length and a relatively short digit V, the high divarication angle with diverging digit bases, the short palm/sole impressions, the relative size of the manus and pes tracks and the trackway pattern with inwardly-directed manus footprints, are characteristic of the ichnogenus *Hyloidichnus* Gilmore, 1927 (e.g., Haubold, 1971; Gand, 1987; Haubold et al., 1995; Gand and Durand, 2006; Mujal et al., 2016; Voigt and Lucas, 2018; Marchetti et al., 2020c).

Hyloidichnus is a common ichnogenus of the Permian, known from:

- USA, from the Cisuralian Hermit Shale Formation (Gilmore, 1927; Marchetti et al., 2020c), Robledo Mountains Formation (Voigt and Lucas, 2015) and Abo Formation (Lucas et al., 2013; Voigt and Lucas, 2017);
- Argentina, from the Cisuralian-Guadalupian Carapacha Formation of the Carapacha Basin (Melchor and Sarjeant, 2004).
- France, from the Cisuralian (Artinskian) Rabejac Formation of the Lodève Basin (Gand, 1987), the Cisuralian (Artinskian-Kungurian) Pélites de Saint Pierre Formation of the Saint-Affrique Basin (Gand, 1993), the Cisuralian of the Blanzy-Le Creusot Basin (Gand, 1981) and the Guadalupian (Wordian-Capitanian) Pelitic Formation of the Le Luc Basin and Pradineaux, Mitan, Muy and La Motte Formation of the Estérel and Bas-Argens basins (Heyler and Montenat, 1980; Demathieu et al., 1992; Gand and Durand, 2006);
- Spain, from the Cisuralian (Kungurian) Sotres Formation of the Cantabrian Mountains (Gand et al., 1997), the Cisuralian (Artinskian) Peranera Formation of the Pyrenean Basin (Voigt and Haubold, 2015; Mujal et al., 2016), and the Cisuralian of the Balearic Islands (Matamales-Andreu et al., 2019);
- Italy, from the Cisuralian (Kungurian) Collio, Pizzo del Diavolo and Tregiovo formations (Marchetti *et al*., 2013; Marchetti *et al*., 2015a-c; Marchetti, 2016);
- Morocco, from the Cisuralian 'Upper Formation' of the Tiddas Basin and Koudiat El-Hamra Formation of the Koudiat El-Hamra Basin (Hmich et al., 2006; Voigt et al., 2011; Zouicha et al., 2020); and the Guadalupian-Lopingian Ikakern Formation of the Argana Basin and Cham-el-Haoua Siltstone Formation of the Marrakech High (Voigt et al., 2010; Hminna et al., 2012; Moreau et al., 2020);
- Niger, from the Guadalupian-Lopingian Moradi Formation (Steyer et al., 2007; Smith et al., 2015);

- Turkey, from the Cisuralian Çakraz Formation of Anatolia (Gand et al., 2011).

The type ichnospecies of *Hyloidichnus* is *H. bifurcatus* Gilmore, 1927 from the Permian Hermit Formation of the Grand Canyon (Arizona, USA). Gilmore (1928) also erected *H. whitei* from the same formation. Later, Haubold (1971) proposed the combinations *H. major* and *H. minor* based on the ichnospecies '*Auxipes*' *major* (Heyler and Lessertisseur, 1963) and '*Auxipes*' *minor* (Heyler and Lessertisseur, 1963), from the Permian Rabejac Formation (Lodève Basin, France). Later, two other ichnospecies were erected, *H. arnhardti* Haubold, 1973 and *H. tirolensis* Ceoloni, Conti, Mariotti and Nicosia, 1986 from Italy. According to Haubold (2000), only *H. bifurcatus* and *H. major* are valid, although they may belong to the same ichnospecies (e.g., Gand and Durand, 2006; Marchetti et al., 2020c). Moreover, *Gilmoreichnus (Hylopus) hermitanus* (Gilmore, 1927) may also be an extramorphological variation of *Hyloidichnus* (Marchetti et al., 2013). Therefore, the relationships between these ichnotaxa need to be further investigated.

The footprints described here, especially GONF-A-04, are also similar to the ichnospecies *Varanopus rigidus* Gand, 1989 (Gand and Durand, 2006), whose holotype comes from Gonfaron (Gand, 1989). However, several authors considered this ichnospecies as invalid because material assigned to *V. rigidus* from the Lodève, Saint-Affrique, Estérel and Bas-Argens basins includes footprints assignable to different ichnotaxa such as other *Varanopus* ichnospecies, *Hyloidichnus* and *Notalacerta* (Voigt et al., 2010; Marchetti et al., 2020b).

Pending a comprehensive revision of *Hyloidichnus* and its possible ichnospecies, we prefer to assign the Gonfaron material studied here to *Hyloidichnus* isp.

5. Track-trackmaker correlation

Hyloidichnus is generally attributed to captorhinomorph eureptiles such as small captorhinines (*Captorhinus*) or large moradisaurines (*Moradisaurus*) depending on the shape and size of the footprints (e.g., Voigt et al., 2010). However, the *Hyloidichnus*-captorhinomorph correlation is not based on synapomorphic characters as in other valid correlations (e.g., large *Ichniotherium cottae-Limnoscelis* of Mujal and Marchetti, 2020; small *I. cottae-Diadectes* and *I. sphaerodactylum-Orobates* of Voigt et al., 2007; *Amphisauropus-Seymouria* of Marchetti et al., 2017; *Pachypes ollieri-Macroleter* of Marchetti et al., 2020a). This is due to the lack of studies on well-preserved *Hyloidichnus* footprints correlated to detailed skeletal reconstructions in a morpho-functional perspective. The good preservation of the footprints from Gonfaron allows us to investigate and to define this track-trackmaker correlation:

Anamniotes such as diadectomorphs (trackmakers of *Ichniotherium*), seymouriamorphs (*Amphisauropus*) and amphibians such as eryopoids (*Limnopus*) have well-ossified, short and distally rounded digits as well as ossified and packed carpus and tarsus, resulting in broad palm and sole impressions (Voigt, 2005; Voigt et al., 2007; Marchetti et al., 2017; Mujal and Marchetti, 2020). This is inconsistent with the clawed and bifurcated digit impressions and the short palm and sole impressions of *Hyloidichnus*.

Parareptiles such as pareiasaurs (trackmakers of large *Pachypes dolomiticus*) are too large to fit with *Hyloidichnus*, whereas smaller pareiasauromorphs (trackmakers of *Pachypes ollieri*) have closely-packed digits and overlapping metatarsals and metacarpals, which are inconsistent with the radiating digit imprints and the large digit divarication angle of *Hyloidichnus* (Marchetti et al., 2020a). Also, their tails were short, whereas continuous tail impressions are commonly observed in trackways of *Hyloidichnus*.

The *Hyloidichnus* footprints from Gonfaron show a wide size range in manus (19 to 49 mm long) and pes tracks (28 to 61 mm long) as well as in trackway parameters (Tabs. 1-3). The body trunk length, based on the glenoacetabular distance, also greatly varies in size, between

292 50 mm to 184 mm (Tab. 4). This suggests different taxa as trackmakers, or individuals of the
293 same taxon at different ontogenetic stages. Among captorhinids, relatively complete
294 appendicular elements are known from *Captorhinus aguti* Cope, 1895 (Holmes, 1977),
295 *Labidosaurus hamatus* Willinston, 1910, *Captorhinikos choazensis* Olson, 1962, *Moradisaurus*
296 *grandis* de Ricqlès and Taquet, 1982 (O'Keefe et al., 2005) and *Romeria prima* (Clark and
297 Caroll, 1973). Even though the skeletal remains of captorhinids date back to the Artinskian–
298 Kungurian and the Gonfaron footprints to the Wordian (showing a discrepancy of at least 4
299 Myr), the wide temporal range of *Hyloidichnus* trackways in the fossil record supports this
300 investigation (Fig. 6). *Captorhinus aguti* fits with the size of the footprints of GONF-A-04. This
301 taxon has been correlated to *Varanopus* by Fichter (1983) and Voigt (2005), mostly based on
302 overall morphology and proportions. Also, the mesotarsal joint described by Holmes (2003)
303 was considered an explanation for the medial-lateral decrease in relief of the *Varanopus* pes
304 imprint. Nevertheless, the medial-lateral decrease in relief occurs also in *Hyloidichnus*, and
305 *Varanopus* shows parallel and overlapping digit base impressions, a feature that is characteristic
306 of parareptiles (Lee, 1997) and is not in agreement with the radiating and separated metatarsals
307 of articulated skeletons of *Captorhinus aguti* (Holmes, 2003 figs. 7-8). Therefore, we consider
308 the attribution of *C. aguti* to *Varanopus* as currently not well supported.

309 *Captorhinus* and *Hyloidichnus* share:

310 - pentadactyl manus and pes;
311 - similar relative lengths of the digits (I<V≤II<III<IV for the pes and the manus) (Tabs.
312 1, 2, 5);
313 - radiating and non-overlapping metatarsals/proximal digit imprints;
314 - clawed digit tips;
315 - similar length ratios between: 1) pes/manus length and metatarsus/metacarpus length
316 and 2) pes/manus foot length and sole/palm impression length (Tabs. 1, 2, 5);

317 - similar length/width ratios of the pes (phalanges + tarsus) and of the manus (phalanges
318 + carpus) (<1 for the manus and ~1 for the pes) (Tabs. 1, 2, 5).
319
320 The carpus of *Captorhinus* comprises 11 elements: the radiale, the intermedium, the
321 ulnare, the pisiform, two centralia and five distal carpals (Fig. 7). The joint between the radius
322 and the radiale is flat, suggesting no flexion between them: the radiale may act as an extension
323 of the radius. The convex joint between the radiale and the lateral centrale permitted a
324 significant medio-lateral rotation. In addition, the ulnare and the intermedium form a single
325 structural unit with a flat joint oriented like a dorsal process (Holmes, 1977), causing probably
326 a concave proximal margin of the palm: this fits with the *Hyloidichnus* manus impressions
327 (Fig. 7). The joints are flat between (1) the ulnare and the ulna, (2) the ulnare and the
328 intermedium, and (3) the ulnare and distal carpals 4 and 5. The ulnare and the intermedium
329 contact both the medial centrale, and the latter contacts only marginally the radius-radiale
330 complex. Thus, the lateral centrale is the element of the carpus that experienced the most
331 tension during movement; this element supports both the radius-radiale complex and the ulna-
332 intermedium-ulnare-medial centrale complex (Holmes, 1977; Marchetti et al., 2017). This
333 also fits with the basal part of the *Hyloidichnus* digit I, II and III imprints of the manus, where
334 the footprint is more deeply-impressed (Fig. 7). The joints between the distal carpals are also
335 flat, allowing very little independent movements; this is consistent with the straight and
336 regularly impressed manus digit bases of *Hyloidichnus* (Figs. 2, 7). A distal process behind
337 metacarpal 3 prevented too much flexion of digits III and IV (Holmes, 1977), suggesting a
338 more stable position and rigid appearance compared to the imprints of digits I and II of
339 *Hyloidichnus*. The phalanges of the manus of *Captorhinus* are proportionally thicker and
340 shorter than those of the pes, with significant ossification at the joints (increasing the distance
341 between the tendon and the joint and thus the flexibility of the digit muscles) (Holmes, 1977).

342 This is also suggested in *Hyloidichnus*, which has relatively shorter and thicker digit imprints
343 and overall deeper manus imprints (with marked impressions of digits I and II) compared to
344 the pes imprints, as also observed by the higher expulsion rims in GONF-A-04 (Fig. 2).

345 The tarsus of *Captorhinus* comprises eight elements: the calcaneus, the astragalus, the
346 centrale and five distal tarsals (Fig. 7). The sole impression of *Hyloidichnus* is smaller than the
347 palm impression, probably due to less distal elements of the tarsus compared to the carpus: this
348 is consistent with *Captorhinus*. The centrale, calcaneus, and astragalus are closely nested,
349 suggesting little movements between these elements. The calcaneus has flat joints with the
350 distal tarsals 4 and 5, while the centrale has convex joints with the distal tarsals 1, 2 and 3
351 (Holmes, 2003). Thus, the flexion is mainly supported by the centrale and occurs at the level of
352 the distal tarsals 1, 2 and 3, which is consistent with the deeper impressions of the digits I to III
353 of the pes in *Hyloidichnus* (Fig 7). The phalanges of the *Captorhinus* pes are long and thin,
354 corresponding to the impressions of the pes digits of *Hyloidichnus*. The pes joints are more
355 ossified than the manus joints which could explain the straight digit impressions of the pes and
356 the lack of mobility relative to the manus. The unguals of *Captorhinus* (and captorhinormophs
357 in general) are poorly preserved. However, they seem thinner and shorter in the pes (Holmes,
358 2003) than in the manus (Holmes, 1977). This seems consistent with the thin and shallow pes
359 digit drag traces preserved within the trackways of *Hyloidichnus* (Figs. 2, 4 and 5). They greatly
360 differ from those of *Amphisauropus* that leave deeper and larger digit drag traces
361 indistinguishable among each other, probably due to the thicker digits and the absence of
362 unguals. Holmes (2003), contra Schaeffer (1941), Fox and Bowman (1966) and Sumida (1989),
363 hypothesised a ‘mesotarsal’ joint in *C. aguti*, the dorsiflexion of which suggests a more
364 pronounced medial impression of the sole at the level of the tarsals 1 to 3; this is again consistent
365 with *Hyloidichnus*.

366 *Labidosaurus* and *Captorhinikos* are larger captorhinids than *C. aguti*. They also show
367 similar manus and pes anatomy with, however, shorter and stubbier distal pedal phalanges,
368 resulting in a relatively shorter and wider pes (Sumida, 1989). Such morphology might be
369 coherent with GONF-G21 and GONF-A-11, where the pes impressions are wider than long.
370 So, *Labidosaurus* and *Captorhinikos* may be considered as potential trackmakers for larger
371 *Hyloidichnus* tracks. Recent phylogenetic studies of captorhinomorphs place *Captorhinikos* as
372 the basalmost Moradisaurinae (Modesto et al., 2019), but its phylogenetic position has often
373 changed, within or out of the Moradisaurinae (de Ricqlès, 1984; Reisz et al., 2011, 2015;
374 Modesto et al., 2014; Liebrecht et al., 2017; Cisneros et al., 2020). The clade *Labidosaurus* +
375 Moradisaurinae is well-supported by all these phylogenetic analyses. Inclusive or stem-
376 Moradisaurinae, with autopodials similar to those of *Captorhinus*, could then be potential
377 trackmakers of relatively large *Hyloidichnus* tracks.

378 The pes of *Moradisaurus* is foreshortened and extremely robust compared to other
379 captorhinids. It has a massive astragalus, larger than that of other captorhinids, and a derived
380 calcaneum (O'Keefe et al., 2005). Nevertheless, the tarsus arrangement is the same as that of
381 other captorhinids, with the only exception being the lack of the distal tarsal 5. The body of
382 *Moradisaurus* is extremely large (its weight was probably more than 300 kg), being inconsistent
383 with the size of the studied tetrapod footprints. The metatarsals and phalanges of the pes,
384 although similar to those of other captorhinids, suffered a proximo-distal compression: this may
385 reflect a shortening of the pes digit imprints, but this is not observed in the studied Gonfaron
386 specimens. The position of the femur may also restrict the rotation and movement of the
387 hindlimb during the step cycle, suggesting an antero-posterior movement only (O'Keefe et al.,
388 2005). This movement of the hindlimb may not leave digit drag traces as curved as seen in the
389 studied *Hyloidichnus* trackways. Therefore, *Moradisaurus* and derived moradisaurines may not
390 be the trackmakers of the *Hyloidichnus* tracks from Gonfaron.

6. Locomotor reconstruction

The locomotor cycle of the hindlimb of *Captorhinus aguti* reconstructed by Holmes (2003), in which the outer digits are first to leave the substrate during the kick-off phase, is generally consistent with an increased medial relief of the pes impression. This is regularly observed in *Hyloidichnus* (e.g., Gand, 1987; Mujal et al., 2020), including small *Hyloidichnus* tracks as those observed on GONF-A-04. It has to be noted that the pes orientation of *Captorhinus* proposed by Holmes (2003) is slightly different from that of *Hyloidichnus.* The absence of a cruro-tarsal joint in *Captorhinus* is in agreement with the semi-plantigrady of the impressions. The shortened impression of the sole then resulted from the impression of the distal tarsus and proximal metatarsus (Holmes, 2003; Voigt, 2005). *Hyloidichnus* manus and pes imprints rarely overlap, and the position of the pes-manus couples is consistent with a sprawling locomotion observed in many present-day tetrapods (Schaeffer, 1941; Brinkman, 1980, 1981; Pardian and Olsen, 1984) and in trace fossils such as *Amphisauropus* and its possible trackmaker *Seymouria* (Marchetti et al., 2017). Holmes (2003) reconstructed the stance phase of the pes of *C. aguti* based on the hindlimb skeleton. However, the following pes swing phase could not be reconstructed due to the absence of some elements. The locomotor cycle of *Captorhinus* has been reconstructed mainly according to skeletal elements, while footprints are rarely used (Holmes, 2003 used them only for imposition of constraints). Reconstruction of the pes swing phase was performed for *Seymouria* thanks to exceptionally preserved *Amphisauropus* tracks and trackways, including continuous digit drag traces (Marchetti et al., 2017). Tracks give important information on the different steps of the locomotion: how the manus/pes leave, arrive and rest on the sediment (stance phase). While other aspects of the step cycle, when the manus/pes are off the substrate (swing phase), are less certain, the presence of digit drag traces allows a rather precise reconstruction of this part of the locomotion (which

cannot be inferred through tracks nor anatomical analyses). The trackways analysed here are consistent with Holmes' analysis on the stance phase, but not demonstrative of all of it. The well-preserved Gonfaron footprint material including trackways and continuous digit drag traces, coupled with the work of Holmes (2003), allows us to propose a reconstruction of the swing phase of *Captorhinus*, for both the pes and the manus.

6.1. Forelimb step cycle

Considering the manus tracks, the deep impression of the digits I, II and III suggests an important role of this manus portion during the stance phase to support the weight of the body. However, to accommodate the change in body weight support to the pre-axial side, digits I, II and III moved from a position almost parallel to the trackway midline to a position almost perpendicular (as represented by the inwards rotated manus tracks). This resulted in more excursion of the humerus than that of the femur to accompany this re-orientation of the digits during the midstride. The position of the manus was then nearly perpendicular relative to the substrate with the digits positioned high above it at the end of the stance phase. Digit dragging is generally more frequent in hindlimbs than forelimbs (Willey et al., 2004; Farlow et al., 2017). However, crocodylians and other reptiles such as the Komodo monitors leave manus digit drag traces because of their lateral excursion of the humerus, almost at 90° to the body trunk (Padian and Olsen, 1984). The absence or shallow impression of digit drag traces associated with the *Hyloidichnus* manus imprints could be due to the more important antero-posterior movement of the elbow compared to crocodylians, which increased the length of the stride with more flexion that prevented digit dragging (Holmes, 1977). This would be in agreement with a more advanced forelimb posture of captorhinids compared to crocodiles. A lifted position of the manus at the end of the stance phase could also be an explanation for the scarcity of manus digit drag traces in *Hylodichnus*. The stance phase of the manus is consistent with the stance phase

441 reconstructed for the pes by Holmes (2003), with an active role of the digits I to III. The swing
442 phase of the manus can be reconstructed thanks to the well-preserved and continuous digit drag
443 traces of GONF-G21 (Fig. 8-I).

444 - *Beginning of the swing phase* (Fig. 8-IA): all digits of the manus have left the substrate.
445 The complex radius/ulna undergoes a rotation of about 90°, so that only the tips of the
446 digits IV and V touch the substrate, leaving continuous digit drag traces. However, the
447 digit drag traces are very thin (and often absent in *Hyloidichnus* trackways), suggesting
448 a position of the digits well above the substrate. The humerus reaches its maximum
449 height with an excursion over 90°;
450 - *Early swing phase* (Fig. 8-IB): almost immediately, the humerus undergoes a rotation
451 of 20° anteriorly, allowing the generation of digit drag traces of digit III (as seen in
452 GONF-G21). The angle with the body axis stays the same;
453 - *Midstride* (Fig. 8-IC): during the midstride, the position of the manus relative to the
454 substrate and of the humerus relative to the body axis does not move (or very slightly)
455 resulting in the absence of an arcuate movement of the digit drag traces of the manus
456 compared to those of the pes;
457 - *End of the swing phase* (Fig. 8-ID): the humerus reaches its lower height with an
458 excursion below 90°. The manus shifts from an inclined to a parallel orientation towards
459 the substrate. This is permitted by a re-orientation of the carpus. The manus is in its
460 medial-most position, leaving the next imprint.

461

462 *6.2. Hindlimb step cycle*

463 The specimens GONF-A-04 and GONF-G21 show continuous digit drag traces, which
464 allow to describe the movement of the pes from one step to the following one (Fig. 8-II). Most
465 of the digit drag traces are represented by three to four curved lines that depart from the pedal

digit impressions II, III, IV and V. The curved line from digit V impression is the longest. It decreases in length from impressions of digit IV to II. This suggests that the digit I and II left the substrate first, while digits III to V kept their position on the substrate, as shown during the midstride and end of stance phase by Holmes (2003). The swing phase is then similar to that of a living alligator where "early in the hindlimb protraction, the distal end of the femur undergoes slight abduction, relative to its position at the end of the stance phase, as it swings forward, the extent of abduction varying among individual alligators" (Farlow et al., 2017, p. 29). This is consistent with the number of digit drag traces in *Hyloidichnus* trackways, which ranges between two and four. The digit drag traces in *Hyloidichnus* and crocodilians trackways (Farlow et al., 2017) consist of similar curved lines, suggesting a similar movement.

- *Beginning of the swing phase* (Fig. 8-IIA): all digits of the pes have left the substrate. The complex tibia/fibula undergoes a rotation of about 90°. Only the tips of digits IV and V touch the substrate, leaving the continuous digit drag traces. The frequency and sharpness of the pes digit drag traces amongst *Hyloidichnus* trackways suggest that the femur is less excursed than the humerus, at 90° relative to the body axis;
- *Early swing phase* (Fig. 8-IIB): the femur undergoes an anterior rotation probably of 20°, corresponding to the best-preserved digit drag traces of digits III, IV and V. Simultaneously to this rotation, the angle of the femur with the body axis diminishes. These re-orientations are marked by an arcuate movement of the digit drag traces towards the outside of the trackway midline (as seen in GONF-A-04). This is not seen in the manus digit drag traces, which are more regular;
- *Midstride* (Fig. 8-IIC): the femur continues its rotation (of about 60° at the end of the midstride) leading to the drag trace of digit II. However, the tip of the digit II pass slightly over the substrate and may not always leave drag traces. During the midstride, digit drag traces of the pes are more rectilinear than those of the manus: this suggests

that the femur has a less prominent excursion than that of the humerus. It is already below 90° relative to the body axis;

- *End of the swing phase* (Fig. 8-IID): the femur reaches its lower height. The pes shifts to a parallel orientation towards the substrate. This is permitted by a re-orientation of the tarsus. The pes is in its medial-most position, leaving the next imprint.

6.3. Tail impression and gait

Deep and wide tail impressions and continuous digit drag traces are rarely observed in *Hyloidichnus* (Gand, 1987). Similar tail impressions and digit drag traces have been observed in the Permian ichnogenus *Erpetopus*, the trackmaker of which is interpreted to be a small reptile (Bernardi and Avanzini, 2011). The exceptional preservation of these features on the studied specimens may be due to differences in gait and substrate, which was probably more water-saturated and muddy (Marchetti et al., 2017, 2019b). Contrary to *Amphisauropus*, where well-impressed and continuous tail traces are associated with digit drag traces and present a significant sinuosity (Marchetti et al., 2017), the *Hyloidichnus* tail impression shows generally a very low sinuosity, except for GONF-A-11. Variations in the sinuosity of the tail impression are observed in present day tetrapods such as crocodilians (Farlow et al., 2017). The nearly rectilinear tail impression in *Hyloidichnus* suggests that its captorhinomorph trackmaker had a lower body sway and spine flexibility than those of the seymouriamorph trackmaker of *Amphisauropus* (Berman et al., 2000; Marchetti et al., 2017). Although, as in *Amphisauropus* trackways, an arcuate movement of the scratches suggests a rather marked lateral movement of the body (Ashley-Ross, 1994; Marchetti *et al.*, 2017). Captorhinomorph eureptiles, alongside seymouriamorphs, could have had a more derived body trunk flexibility in comparison with earlier tetrapods (Pierce et al., 2013; Marchetti et al., 2017). The body and tail of captorhinomorphs might also have been more lifted than those of seymouriamorphs. A more

distal part part of the tail may have been impressed (which was thinner and rectilinear because less subject to the body sway). A subrectilinear tail impression has also been observed in *Dimetropus*, correlated to pelycosaur-grade synapsids (Voigt, 2005). Variations in the width of the tail impression in correspondence with pes-manus couples suggest a slight change in the orientation of the tail during walking, or a slight lowering-rising of the body (Avanzini and Renesto, 2002). Although such slight variations are seen in GONF-A-04, they are not marked enough to suggest a gait with "brief regular spurts" (Avanzini and Renesto, 2002 p. 57). The tail impression of GONF-A-04 is continuous, suggesting that vertical movement was almost absent (Bernardi and Avanzini, 2011; Marchetti et al., 2017). The tail impression is wide and well-marked in specimens GONF-A-04, GONF-A-11 and GONF-G21. This suggests a relatively large and long tail, touching the ground during progression. The steepness and location of the expulsion rims of the tail impression, opposite to the pes-manus couples and in its inner side, (Figs. 9, 10) suggest a lateral movement in the same direction of the head and opposite to the trunk. Such lateral movement of the body is also seen in seymouriamorphs (Marchetti et al., 2017).

However, there are slight differences in the relative depth pattern between trackways GONF-A-04 and GONF-A-11 (Fig. 9). This could be linked to slightly different gait as well as different rheological conditions of the substrate. The two trackways are very different in size (pes and manus imprints in GONF-A-11 are nearly two to three times larger than those of GONF-A-04). As discussed above, different captorhinomorph taxa as trackmakers cannot be discarded, but the manus and pes skeletons of captorhinomorphs are extremely conservative and cannot explain such differences. An evolution of the locomotion through ontogenetic stages of the skeleton in captorhinomorph would also be unlikely. A limited skeletal ossification indeed characterizes many eureptilian neonates (age class that express attributes mostly influenced by pre-parturitive development environment such as the egg or the egg-nest,

Morafka et al., 2000), but the size of the trackmaker of GONF-A-04 (50 mm) compared to size of the trackmaker of GONF-A-11 (175 mm), would rather indicate a juvenile form. Unfortunately, juvenile captorhinomorph skeletons are not known. The following discussion will therefore concentrate on gait and substrate. High speed is known to affect the trackways of reptiles and amphibians, potentially causing: primary overstepping of the pes to the manus, absence of a tail impression, high pace angulation, high stride length/foot length (SL/FL) ratio, position of the digit V of the pes nearly perpendicular to the trackway midline, high rotation of the manus and pes in respect to the trackway midline and a Y-shaped digit tip impressions of the pes imprints (Peabody, 1956; Irschick and Jayne, 1999; Dietrich and Gardner, 2004; Dietrich, 2008). Both, GONF-A-04 and GONF-A-11 show a tail impression inconsistent with high-speed locomotion but rather a walking-type locomotion (Avanzini and Renesto, 2002; Pierce et al., 2013; Marchetti et al., 2017; Mujal et al., 2017). However, it is not incompatible with a higher speed of one trackmaker relative to the other. The GONF-A-04 trackway has a pace angulation lower than that of GONF-A-11, but a higher SL/FL ratio with a higher inter-pes and inter-manus distance; the rotation of the manus and pes tracks in respect to the trackway midline is higher in GONF-A-04 than in GONF-A-11 with a higher divarication of the digit V (Tables 1, 2). In addition, the morphology of the digit tips of GONF-A-04 present a Y-shaped impression but not in GONF-A-11, where the digit tip impression is directed laterally, suggesting a slower gait (Peabody, 1956). A slightly higher locomotion gait of the trackmaker of GONF-A-04 is then plausible. GONF-A-04 shows a rectilinear tail impression, whereas GONF-A-11 shows a sinuous tail impression. In GONF-G-21, which also presents a nearly rectilinear tail impression, the pace angulations, SL/FL ratio, the inter-manus distance and divarication of the pes are similar to those of GONF-A-04 (Tables 1, 3, 4), although the footprint and supposed trackmaker size are closer to those of GONF-A-11. So, a lower tail sinuosity may be coherent with a slightly higher locomotion gait. Moreover, the substrate of GONF-A-04 and

566 GONF-A-11 was quite different: alongside GONF-A-04 are found traces of bioturbation and
567 burrows and the tracks present high expulsion rims and a more defined shape of the imprints,
568 digit drag traces and tail impressions: this suggests a water-saturated substrate, with sufficient
569 cohesiveness to register small details. In GONF-A-11, the substrate would have been drier, as
570 none of those features are recovered from the slab. Nevertheless, the relative depth pattern of
571 both manus and tracks of both trackways seem to show a medial-median functional prevalence.
572 This is consistent with the fact that rheology does not affect the trackmaker´s functional
573 morphology: the relative depth patterns are the same for each ichnotaxon across different
574 substrates, Mujal et al., 2020). As in the studied material, speed also seems not to have effect
575 on the functional prevalence of the trackmaker. Trackways showing a conclusive high gait
576 should be analysed to eventually confirm this hypothesis.

577

578 **7. Conclusions**

579 The discovery of new exceptionally well-preserved specimens from Gonfaron (Var,
580 France), together with the revision of those from the Burgundy University collections, allows
581 to precise the ichnological description of *Hyloidichnus* and to better understand its potential
582 trackmakers, as well as their locomotion style. The correlation between *Hyloidichnus* and
583 *Captorhinus* (and captorhinomorphs with similar autopodia) is hence proposed for the first time
584 in a synapomorphy-based approach.

585 The exceptional preservation of continuous digit drag traces and tail impressions
586 allowed a detailed review of the captorhinomorph locomotion. The stance phase of the pes of
587 captorhinomorphs is coherent with *Hyloidichnus* trackways, suggesting a greater role than
588 previously thought of the manus during the propulsion of the body. The swing phase of both
589 manus and pes for captorhinomorphs has been reconstructed for the first time. A possible

590 marked body trunk flexibility has been highlighted in captorhinomorphs, compared with other
591 Permian tetrapods. However, the tail impression, except for one specimen, suggests moderate
592 body sway. A new hypothesis of a “lifted body” in captorhinomorphs is thus proposed.

593 These trackways finally permitted detailed observations on different locomotion gait.
594 Even though high speed locomotion is not represented, slight changes in speed observed from
595 the *Hyloidichnus* trackways parameters have been documented. Two interesting outcomes,
596 which need further investigation, are: 1) the correlation between the shape of the tail impression
597 in response to the locomotion gait and 2) the absence of impact of speed and rheology on the
598 functional prevalence of autopodia.

599 Gonfaron is a locality recently re-opened in the Permian of France (Var). Together with
600 new insect specimens recently described, these new discoveries also show that Gonfaron is an
601 important locality to better understand the Permian faunas and their associated
602 palaeoenvironements of France and Europe. This acquires even more importance due to the
603 middle Permian age of this site, since low-palaeolatitude fossil-bearing localities of this age are
604 rare.

605

606 **Acknowledgements**

607 We thank the Mayor of Gonfaron for authorizations to collect fossils, the Maison de la Nature
608 (Les Mayons) for accommodations, I. van Waveren (Natural History Museum Leiden), J.
609 Fortuny (ICP), Stanislav Stamberg (Eastern Bohemian Museum Czech Republic), G. Lemaitre
610 (Phylogenia Association), G. Gand (Dijon University), M. Durand (Nancy University), T.
611 Arbez (Ottawa University), and the excavation team (M. Raymond, M. Ughetto, X. Pouly, V.
612 Blondel, M. Denis) for their help in the field. We thank E. Fara and J. Thomas for the access to
613 the Dijon University collection. This research was supported by the interdisciplinary programs

RedPerm I and II, ATM MNHN, LabEx, and Projet Fédérateur MNHN attributed to J-S.S., R.G, and A.N. The Alexander von Humboldt Foundation and the Bundesministerium für Bildung und Forschung (BMBF) for the BROMACKER Project 2020-2025 financed LM. This work received support from the CERCA programme (ICP) from the Generalitat de Catalunya. We acknowledge the reviews of Spencer G. Lucas, Sebastian Voigt and Hendrik Klein and of the editors Prof. Howard Falcon-Lang and Prof. Thomas J. Alego, which helped to improve a previous version of the manuscript.

References

Ashley-Ross, M., 1994. Hindlimb kinematics during terrestrial locomotion in a salamander (*Dicamptodon tenebrosus*). J. Exp. Biol. 193, 255-283.

Avanzini, M., Renesto, S., 2002. A review of *Rhynchosauroides tirolicus* Abel, 1926 ichnospecies (Middle Triassic: Anisian-Ladinian) and some inferences on *Rhynchosauroides* trackmaker. Riv. Ital. Paleontol. S. 108, 51–66.

Berman, D.S., Henrici, A.C., Sumida, S.S., Martens, T., 2000. Redescription of *Seymouria sanjuanensis* (Seymouriamorpha) from the Lower Permian of Germany based on complete, mature specimens with a discussion of paleoecology of the Bromacker locality assemblage. J. Vertebr. Palentol. 20, 253-268.

Bernardi, M., Avanzini, M., 2011. Locomotor behavior in early reptiles: insights from an unusual *Erpetopus* trackway. J. Paleontol. 85, 925-929.

Brinkman, D., 1980. The hind limb step cycle of *Caiman sclerops* and the mechanics of the crocodile tarsus and metatarsus. Can. J. Zool. 58, 2187-2200.

636 Brinkman, D., 1981. The hindlimb step cycle of *Iguana* and primitive reptiles. J. Zool. 193, 91-
637 103.

638 Buchwitz, M., Voigt, S., 2018. On the morphological variability of *Ichniotherium* tracks and
639 evolution of locomotion in the sistergroup of amniote. PeerJ 6, e4346.

640 Butts, E., 1891. Recently discovered foot-prints of the Amphibian age, in the Upper Coal
641 Measure group of Kansas City, Missouri. *Kansas City Scientist* 5, 17-19.

642 Ceoloni, P., Conti, M.A., Mariotti, N., Nicosia, U., 1986. New Late Permian tetrapod footprints
643 from southern Alps. Mem. Soc. Geol. Ital. 34, 45-66.

644 Cisneros, J.C., Angielczyk, K., Kammerer, C.F., Smith, R.M.H., Fröbisch, J., Marsicano, C.A.,
645 Richter, M., 2020. Captorhinid reptiles from the lower Permian Pedra de Fogo Formation, Piauí,
646 Brazil: the earliest herbivorous tetrapods in Gondwana. PeerJ 8: e8719. doi: 10.7717/peerj.8719

647 Clark, J., Caroll, R.L., 1973. Romeriid reptiles from the Lower Permian: Harv. Univ., Mus.
648 Comp. Zool. Bull. 144, 353-407.

649 Cope, E.D., 1895. The reptilian order Cotylosauria. Proc. Am. Philos. Soc. 34, 436-457.

650 Demathieu, G., Gand, G., Toutin-Morin, N., 1992. La palichnofaune des bassins permiens
651 provençaux. Geobios 25, 19-54.

652 Dietrich, C., 2008. Millions of reptile tracks – Early to Middle Triassic carbonate tidal flat
653 migration bridges of Central Europe – reptile immigration into the Germanic Basin.
654 Palaeogeogr. Palaeoclimatol. Palaeoecol. 259, 410-423.

655 Dietrich C.G., Gardner, A.S., 2004. Lacertilian trackway experiments in the carbonate tidal flats
656 of All Dabb'iya, western Abu Dhabi, U.A.E. Triubulus 13, 23-28.

Durand, M., 2008. Permian to Triassic continental successions in southern Provence (France): an overview. Boll. Soc. Geol. Ital. 127, 697-716.

Falkingham, P.L., 2012. Acquisition of high resolution three-dimensional models using free, open-source, photogrammetric software. Palaeontol. Electronica 15, 15.

Farlow, J.O., Robinson, N.J., Kumagai, C.J., Paladino, F.V., Falkingham, P.L., Elsey, R.M., Martin, A.J., 2017. Trackways of the American crocodile (*Crocodylus acutus*) in Northwestern Costa Rica: implications for crocodylian ichnology. Ichnos. doi: 10.1080/10420940.2017.1350856.

Fichter, J., 1983. Tetrapodenfährten aus dem saarpfälzischen Rotliegenden (Ober-Karbon-Unter-Perm; SW-Deutschland), Teil II: Die Fährten der Gattungen *Foliipes*, *Varanopus*, *Ichniotherium*, *Dimetropus*, *Palmichnus*, *Phalangichnus*, cf. *Chelichnus*, cf. *Laoporus* und *Anhomoiichnium*. Mainz. Naturwiss. Arch. 21, 125-186.

Fox, R.C., Bowman, M.C., 1966. Osteology and relationships of *Captorhinus aguti* (Cope) (Reptilia: Captorhinomorpha). Univ. Kansas Paleontol. Contrib. Vertebrata. 11, 1-79.

Gand, G., 1981. Découverte de traces de reptiles cotylosauriens dans le Permien du bassin de Blanzy-Le Creusot (Saône-et-Loire, France). Une étape dans la succession des palichnofaune de vertébrés tétrapodes. CR. Acad. Sci. Ser III. 292, 163-167.

Gand, G., 1987. Les traces de vertébrés tétrapodes du Permien français, paléontologie, stratigraphie, paléoenvironnements. (PhD thesis). Université de Bourgogne, Dijon (341 pp.)

Gand, G., 1989. *Varanopus rigidus* : une nouvelle ichnoespèce de vertébré tétrapode du Permien français attribuable à des captorhinomorpha ou à des procolophonoidea. Geobios 22, 277-291.

679 Gand, G., 1993. La palichnofaune de vertébrés tétrapodes du bassin permien de Saint-Affrique
680 (Aveyron) : comparaisons et conséquences stratigraphiques. Géol. France 1, 41-56.

681 Gand, G., Garric, J., Demathieu, G., Ellenberger, P., 2000. La palichnofaune du Permien
682 Supérieur du Bassin de Lodève (Languedoc – France). Palaeovertebr. 29, 1-81.

683 Gand, G., Durand, M., 2006. Tetrapod footprint ichno-associations from French Permian
684 basins. Comparisons with other Euramerican ichnofaunas. In: Lucas, S.G., Cassinis, G.,
685 Schneider, J.W. (Eds.), Non-Marine Permian Biostratigraphy and Biochronology. Geological
686 Society of London, Special Publications 265, pp. 157-177.

687 Gand, G., Kerp, H., Parsons, C., Martinez-García, E., 1997. Palaeoenvironmental and
688 stratigraphic aspects of animal traces and plant remains in Spanish Permian red beds (Peña
689 Sagra, Cantabrian Moutains, Spain). Geobios 30, 295-318.

690 Gand, G., Tüysüz, O., Steyer, J.-S., Allain, R., Sakinç, M., Sanchez, S., Şengor, A.M.C., Sen,
691 S., 2011. New Permian tetrapod footprints and macroflora from Turkey (Çakraz Formation,
692 northwestern Anatolia): biostratigraphic and palaeoenvironmental implications. CR Palevol 10,
693 617-625.

694 Garrouste, R., Lapeyrie, J., Steyer, J.-S., Giner, S., Nel, A., 2017. Insects in the Red Middle
695 Permian of Southern France: first Protanisoptera (Odonatoptera) and new Caloneurodea
696 (Panorthoptera), with biostratigraphical implications. Hist. Biol. 30, 546-553.

697 Gilmore, G.W., 1927. Fossil footprints from the Grand Canyon: Second contribution. Smithson.
698 Misc. Collect. 80, 1-78.

699 Gilmore, G.W., 1928. Fossil footprints from the Grand Canyon: Third contribution. Smithson.
700 Misc. Collect. 80, 1-21.

Hasiotis, S.T., Platt, B.F., Hembree, D.I., Everheart, M.J., 2007. The trace-fossil record of vertebrates. In: III Miller (Ed.), Trace Fossils: Concepts, Problems, Prospects. Elsevier, pp. 196-218.

Haubold, H., 1971. Ichnia amphibiorum et Reptiliorum fossilium. In : Kuhn, O. (Ed.), Handbuch der Paläoherpetologie. 18 Gustav Fischer Verlag, Stuttgart and Portland (124 pp.).

Haubold, H., 1973. Die Tetrapodenfährten aus dem Perm Europas. Freiberger Forsch.-Hefte C. 285, 5-55.

Haubold, H., 2000. Tetrapodenfährten aus dem Perm – Kenntnisstand und progress 2000. Hallesches Jahrb. Geowiss. B. 22, 1-16.

Haubold, H., Lockley, M.G., Hunt, A.P., Lucas, S.G., 1995. Lacertoid footprints from Permian dune sandstones, Cornberg and De Chelly Sandstones. N. M. Mus. Nat. Hist. Sci. Bull. 6, 235-244.

Heyler, D., Montenat, C., 1980. Traces de pas de vertébrés du Permien du Var. Intérêt biostratigraphique. Bull. Mus. Natl. Hist. Nat. 4C. 4, 407-451.

Heyler, D., Lessertisseur, J., 1963. Pistes de tétrapodes permiens dans la région de Lodève, Hérault. Mém. Mus. Natl. Hist. Nat. S. C 11, 125-220.

Hmich, D., Schneider, J.W., Saber, H., Voigt, S., El Wartiti, M., 2006. New continental Carboniferous and Permian faunas of Morocco: implications for biostratigraphy, palaeobiogeography and palaeoclimate. In: Lucas, S.G., Cassinis, G., Schneider, J.W. (Eds.), Non-Marine Permian Biostratigraphy and Biochronology. Geological Society of London, Special Publications 265, pp. 297-324.

722 Hminna, A., Voigt, S., Saber, H., Schneider, J.W., Hmich, D., 2012. On a moderately diverse
723 continental ichnofauna from the Permian Ikakern Formation (Argana Basin, Western High
724 Atlas, Morocco). J. Afr. Earth Sci. 68, 15-23.

725 Holmes, R.B., 1977. The osteology and musculature of the pectoral limb of small captorhinids.
726 J. Morphol. 152, 101-140.

727 Holmes, R.B., 2003. The hind limb of *Captorhinus aguti* and the step cycle of basal amniotes.
728 Can. J. Earth Sci. 40, 515-526.

729 Irschick, D.J., Jayne, B.C., 1999. Comparative three-dimensional kinematics of the hindlimb
730 for high-speed bipedal and quadrupedal locomotion of lizards. J. Exp. Biol. 202, 1047-1065.

731 Lee, M.S.Y., 1997. The evolution of the reptilian hindfoot and the homology of the hooked fifth
732 metatarsal. J. Evolution Biol. 10, 253-263.

733 Leonardi, G., 1987. Glossary and Manual of Tetrapod Footprint Paleoichnology. Departamento
734 Nacional de Produção Mineral, Brasilia (117 pp.).

735 Liebrecht, T., Fortuny, J., Galobart, À, Müller, J., Sander, P.M., 2017. A large multiple-tooth-
736 rowed captorhinid reptile (Amniota: Eureptilia) from the Upper Permian of Mallorca (Balearic
737 Islands western Mediterranean). J. Vertebr. Paleontol. 37, e1251936.

738 Lucas, S.G., Krainer, K., Chaney, D.D., Dimichele, W.A., Voigt, S., Berman, D.S., Henrici,
739 A.C. 2013. The Lower Permian Abo Formation in Central New Mexico. N. M. Mus. Nat. Hist.
740 Sci. Bull. 59, 161-180.

741 Marchetti, L., Avanzini, M., Conti, M.A., 2013. *Hyloidichnus bifurcatus* Gilmore, 1927 and
742 *Limnopus heterodactylus* (King, 1845) from the Early Permian of Southern Alps (N Italy): A
743 new equilibrium in the Ichnofauna. Ichnos 20, 202-213.

744 Marchetti, L., Ronchi, A., Santi, G., Schirolli, P., Conti, M.A., 2015a. Revision of a classic site
745 for the Permian tetrapod ichnology (Collio Formation, Rompia and Caffaro valleys, N. Italy),
746 new evidences for the radiation of captorhinomorph footprints. Palaeogeogr. Palaeoclimatol.
747 Palaeoecol. 433, 140-155.

748 Marchetti, L., Ronchi, A., Santi, G., Voigt, S., 2015b. The Gerola Valley site (Orobic Basin,
749 Northern Italy): a key for understanding late Early Permian tetrapod ichnofaunas. Palaeogeogr.
750 Palaeoclimatol. Palaeoecol. 439, 97-116.

751 Marchetti, L., Forte, G., Bernardi, M., Wappler, T., Hartkpf-Fröder, C., Krainer, K.,
752 Kustatscher, E., 2015c. Reconstruction of a Late Cisuralian (Early Permian) floodplain lake
753 environment: Palaeontology and sedimentology of the Tregiovo Basin (Trentino-Alto Adige,
754 Northern Italy). Palaeogeogr. Palaeoclimatol. Palaeoecol. 440, 180-200.

755 Marchetti, L., 2016. New occurrences of tetrapod ichnotaxa from the Permian Orobic Basin
756 (Northern Italy) and critical discussion of the age of the ichnoassociation. Pap. Palaeontol. 2,
757 363-386.

758 Marchetti, L., Mujal, E., Bernardi, M., 2017. An unusual *Amphisauropus* trackway and its
759 implication for understanding seymouriamorph locomotion. Lethaia **50**, 162-174.

760 Marchetti, L., Klein, H., Buchwitz, M., Ronchi, A., Smith, R.M., De Klerk, W.J., Sciscio, L.,
761 Groenewald, G.H., 2019a. Permian-Triassic vertebrate footprints from South Africa:
762 Ichnotaxonomy, producers and biostratigraphy through two major faunal crises. Gondwana
763 Res. 72, 139-168.

764 Marchetti, L., Belvedere, M., Voigt, S., Klein, H., Castanera, D., Díaz-Martínez, I., Marty, D.,
765 Xing, L., Feola, S., Melchor, R.N., Farlow, J.O., 2019b. Defining the morphological quality of

766 fossil footprints. Problems and principles of preservation in tetrapod ichnology with examples
767 from the Palaeozoic to the present. Earth Sci. Rev. 193, 109-145.

768 Marchetti, L., Voigt, S., Mujal, E., Lucas, S.G., Francischini, H., Fortuny, J., Santucci, V.L.,
769 2020a. Extending the footprint record of Pareiasauromorpha to the Cisuralian: earlier
770 appearance and wider palaeobiogeography of the group. Pap. Paleontol. doi:
771 10.1002/spp2.1342.

772 Marchetti, L, Voigt, S., Lucas, S. G., Stimson, M. R., King O. A., Calder, J. H., 2020b.
773 Footprints of the earliest reptiles: *Notalacerta missouriensis* – Ichnotaxonomy, potential
774 trackmakers, biostratigraphy, palaeobiogeography and palaeoecology. Ann. Soc. Geol. Pol., 90
775 doi: 10.14241/asgp.2020.13.

776 Marchetti, L., Francischini, H., Lucas, S.G., Voigt, S., Hunt, A.P., Santucci, V.L., 2020c.
777 Paleozoic vertebrate ichnology of Grand Canyon National Park. In: Santucci, V.L., Tweet,
778 J.S.(Eds.), Grand Canyon National Park: Centennial paleontological resource inventory.
779 National Park Service, Fort Collins, Colorado, pp. 333-379.

780 Matamales-Andreu, R., Fortuny, J., Mujal, E., Galobart, À., 2019. Tetrapod tracks from the
781 Permian of Mallorca (western Mediterranean): preliminary data, biostratigraphic and
782 biogeographic inferences. In: The Palaeontological Association, 63rd annual meeting, 15th–
783 21st December 2019: 107.

784 Melchor, R.N., Sarjeant, W.A.S., 2004. Small amphibian and reptile footprints from the
785 Permian Carapacha basin, Argentina. Ichnos 11, 57-78.

786 Modesto, S., Smith, R.M., 2001. A new Late Permian captorhinid reptile: a first record from
787 the South African Karoo. J. Vertebr. Paleontol. 21, 405-409.

788 Modesto, S.P., Lamb, A.J., Reisz, R.R., 2014. The captorhinid reptile *Captorhinikos valensis*
789 from the lower Permian Vale Formation of Texas and the evolution of herbivory in eureptiles.
790 J. Vertebr. Paleontol. 34, 291-302.

791 Modesto, S.P., Richards, C.D., Ide, O., Sidor, C.A., 2019. The vertebrate fauna of the Upper
792 Permian of Niger – X. The mandible of the captorhinid reptile *Moradisaurus grandis*. J.
793 Vertebr. Paleontol. 38, e1531877.

794 Morafka, D.J., Spangenberg, E.K., Lance, V.A., 2000. Neonatalogy of the reptiles. Herpetol.
795 Monogr. 14, 353-370.

796 Moreau, J.-D., Benaouiss, N., Tourani, A., Steyer, J.-S., Laurin, M., Peyer, K., Béthoux, O.,
797 Aouda, A., Jalil, N.-E., 2020. A new ichnofauna from the Permian of the Zat Valley in the
798 Marrakech High Atlas of Morocco. J. Afr. Earth. Sci. 172, 103973.

799 Mujal, E., Marchetti, L., 2020. *Ichniotherium* tracks from the Permian of France, and their
800 implications for understanding the locomotion and palaeobiogeography of large
801 diadectomorph. Palaeogeogr. Palaeoclimatol. Palaeoecol. 547, 109698. doi :
802 10.1016/j.palaeo.2020.109698

803 Mujal, E., Schoch, R. R., 2020. Middle Triassic (Ladinian) amphibian tracks from the Lower
804 Keuper succession of southern Germany: implications for temnospondyl locomotion and track
805 preservation. Palaeogeogr. Palaeoclimatol. Palaeoecol. 543, 109625. doi:
806 10.1016/j.palaeo.2020.109625

807 Mujal, E., Fortuny, J., Oms, O., Bolet, A., Galobart, À., Anadón, P., 2016. Palaeoenvironmental
808 reconstruction and early Permian ichnoassemblage from the NE Iberian Peninsula (Pyrenean
809 Basin). Geol. Mag. 153, 578-600.

Mujal, E., Fortuny, J., Bolet, A., Oms, O., López, J.Á., 2017. An archosauromorph dominated ichnoassemblage in fluvial settings from the late Early Triassic of the Catalan Pyrenees (NE Iberian Peninsula). PLoS ONE 12, e0174693. https://doi.org/10.1371/journal.pone.0174693.

Mujal, E., Marchetti, L., Schoch, R.R., Fortuny, J., 2020. Upper Paleozoic to Lower Mesozoic tetrapod ichnology revisited: photogrammetry and relative depth pattern inferences on functional prevalence of autopodia. Front. Earth Sci. 8, 248.

O'Keefe, F.R., Sidor, C.A., Larsson, H.C., Maga, A., Ide, O., 2005. The vertebrate fauna of the Upper Permian of Niger-III, morphology and ontogeny of the hindlimb of *Moradisaurus grandis* (Reptilia, Captorhinidae). J. Vertebr. Paleontol. 25, 309-319.

Olson, E.C., 1962. Permian vertebrates from Oklahoma and Texas, Part II. The osteology of *Captorhinikos chozaensis* Olson. Okla. Geol. Surv. Circ. 59, 49-68.

Olson, E.C., Barghusen, H., 1962. Permian vertebrates from Oklahoma and Texas (Vol. 2). University of Oklahoma (68 pp.).

Padian, K., Olsen, P.E. Footprints of the Komodo monitor and the trackways of fossil reptiles. Copeia 3, 662-671.

Peabody, F.E., 1948. Reptile and amphibian trackways from the Lower Triassic Moenkopi Formation of Arizona and Utah. University of California Publications. Bull. Depart. Geol. Sci. 27, 295-468.

Peabody, F.E., 1956. Gilmore's split-toed footprint from the Grand Canyon Hermit Shale Formation.: Plateau, Univ. California **29**, 41-43.

Pierce, S.E., Ahlberg, P.E., Hutchinson, J.R., Molnar, J.L., Sanchez, S., Tafforeau, P., Clack, J.A., 2013. Vertebral architecture in the earliest stem tetrapods. Nature 494, 226.

Reisz, R.R., Liu, J., Li, J., Müller, J., 2001. A new captorhinid reptiles *Gansurhinus qingtoushanensis* gen. et sp. nov., from the Permian of China. Naturwiss. 98, 435-441.

Reisz, R.R., LeBlanc, A.R.H., Sidor, C.A., Scott, D., May, W. 2015. A new captorhinid reptile from the lower Permian of Oklahoma showing remarkable dental and mandibular convergence with microsaurian tetrapods. Sci. Nature 102, 50. doi: 10.1007/s00114-015-1299-y.

Ricqlès, A.de., 1984. Remarques systématiques et méthodologiques pour server à l'étude de la famille des Captorhinides (Reptilia, Cotylosauria, Captorhinimorpha). Ann. Paléontol. 70, 18-21.

Ricqlès, A.de., Taquet, P., 1982. La faune de vertébrés du Permien supérieur du Niger. I. Le captorhinomorphe *Moradisaurus grandis* (Reptilia, Cotylosauria). Le crâne. Ann. Paléontol. 68, 33-106.

Romano, M., Citton, P., Nicosia, U., 2016. Corroborating trackmaker identification through footprint functional analysis: the case study of *Ichniotherium* and *Dimetropus*. Lethaia 49, 102-116.

Schaeffer, B., 1941. The morphological and functional evolution of the tarsus in amphibians and reptiles. Bull. Am. Mus. Nat. Hist. 78, 398-472.

Smith, R.M., Sidor, C.A., Tabor, N.J., Steyer, J.-S., 2015. Sedimentology and vertebrate taphonomy of the Moradi Formation of northern Niger: A Permian wet desert in the tropics of Pangeae. Palaeogeogr. Palaeoclimatol. Palaeoecol. 440, 128-141.

Steyer, J.-S., Gand, G., Smith R.M., Sidor, C.A., Tabor, N., 2007. The first tetrapod trackways from the Paleozoic of West Africa: one step towards reconstructing the landscape of Central Pangea. J. Vertebr. Paleontol. 27, 152A.

854 Sumida, S.S., 1989. The appendicular skeleton of the Early Permian genus *Labidosaurus*
855 (Reptilia, Captorhinomorpha, Captorhinidae) and the hind limb musculature of captorhinid
856 reptiles. J. Vertebr. Paleontol. 9, 295-313.

857 Voigt, S., 2005. Die Tetrapodenichnofauna des kontinentalen Oberkarbon und Perm im
858 Thüringer Wald: Ichnotaxonomie, Paläoökologie und Biostratigraphie (PhD thesis). Martin-
859 Luther Universität Halle-Wittenberg, Göttingen (179 pp).

860 Voigt, S., Lucas, S.G., 2015. Permian tetrapod ichnodiversity of the Prehistoric Trackways
861 National Monument (south-central New Mexico, U.S.A.). N. M. Mus. Nat. Hist. Sci. Bull. 65,
862 153-167.

863 Voigt, S., Lucas, S.G., 2017. Early Permian tetrapod footprints from central New Mexico. N.
864 M. Mus. Nat. Hist. Sci. Bull. 77, 333-352.

865 Voigt, S., Lucas, S.G., 2018. Outline of a Permian tetrapod footprint ichnostratigraphy. In:
866 Lucas, S.G. and Zhen, Z. (Eds.), The Permian Timescale. Geological Society of London,
867 Special Publication 450 pp. 387-404.

868 Voigt, S., Berman, D.S., Henrici, A.C., 2007. First well-established track-trackmaker
869 association of Paleozoic tetrapods based on *Ichniotherium* trackway and diadectid skeletons
870 from the Lower Permian of Germany. J. Vertebr. Paleontol. 27, 553-570.

871 Voigt, S., Hminna, A., Saber, H., Schneider, J.W., Klein, H., 2010. Tetrapod footprints from
872 the uppermost level of the Permian Ikakern Formation (Argana Basin, Western High Atlas,
873 Morocco). J. Afr. Earth Sci. 57, 470-478.

874 Voigt, S., Lagnaoui, A., Hminna, A., Saber, H., Schneider, J.W., 2011. Revisional notes on the
875 Permian tetrapod ichnofauna from the Tiddas Basin, central Morocco. Palaeogeogr.
876 Palaeoclimatol. Palaeoecol. 302, 474-483.

877 Willey, J.S., Biknevicius, A.R., Reilly, S.M., Earls, K.D. 2004. The tale of the tail: limb
878 function and locomotor mechanics in *Alligator mississippiensis*. J. Exp. Biol. 207, 553-563.

879 Willinston, S.W., 1910. The skull of *Labidosaurus*. Am. J; Anat. 10, 69-84.

880 Zouicha, A., Voigt, S., Saber, H., Marchetti, L., Hminna, A., El Attari, A., Ronchi, A.,
881 Schneider, J.W., 2020. First record of permian continental trace fossils in the Jebilet Massif,
882 Morocco. J. Afr. Earth. Sci. 173, 104015.

883

884 **Table 1.** Parameters of the pes imprints of *Hyloidichnus.* FL: foot length (mm), FW: foot width
885 (mm), I-V: digit number, L: digits length (mm), div: digits divarication (degrees).

Specimen	**FL**	**FW**	**I-L**	**II-L**	**III-L**	**IV-L**	**V-L**	**div I/II**	**div II/III**	**div III/IV**	**div IV/V**	**div**
GONF-A-04	28	25	3.6	4.95	7.2	9	4.5	32	30	35	75	172
GONF-G20	53.3	?46.7	18.7	22.7	29.3	32	18.7	33	40	45	39	154
GONF-G21	44.1	51.2	17.6	21.2	28.2	33.5	19.4	45	28	32	35	140
GONF-A-11	61	75	15	24	30	36	25	50	35	40	53	178

886

887 **Table 2.** Parameters of the manus imprints of *Hyloidichnus.* FL: foot length (mm), FW: foot
888 width (mm), I-V: digit number, L: digits length (mm), div: digits divarication (degrees).

Specimen	**FL**	**FW**	**I-L**	**II-L**	**III-L**	**IV-L**	**V-L**	**div I/II**	**div II/III**	**div III/IV**	**div IV/V**	**div**
GONF-A-04	19.2	22	2.25	3.6	4.5	5.4	3.6	30	55	19	50	154
GONF-G20	30.4	48	12.8	19.2	22.4	25.6	9.6	36	43	60	38	177
GONF-G21	35.3	42.4	14.1	15.9	19.4	26.4	12.4	50	45	23	34	152
GONF-A-11	61	48	17	19	27	29	15	50	38	32	53	173

889

Table 3. Trackway parameters. SLp: pes stride length (mm), PLp: pes pace length (mm), Pap: pes pace angulation (degrees), PWp: pes width of pace (mm), Lp-p: pes length of pace (mm), dist ip: distance interpes (mm), divp : pes divarication (degrees), SLm: manus stride length (mm), PLm: manus pace length (mm), Pam: manus pace angulation (degrees), PWm: manus width of pace (mm), Lp-m: manus length of pace (mm), dist im: distance intermanus (mm), divm : manus divarication (degrees).

Specimen	SLp	PLp	Pap	PWp	Lp-p	dist ip	div-p	SLm	PLm	Pam	PWm	Lp-m	dist im	div-m
GONF-A-04	108	78.4	85	49.5	45	38.7	80	101.7	78.75	95	45	56.7	49.5	120
GONF-G20		80		104	88	52.8	50	240	136	120	72	352	24	130
GONF-G21	158.8	123.5	80	112.9	79.4	60	80	155.3	114.7	85	97	70.6	49.4	80
GONF-A-11		21		98	18	20	65	130	19.5	130	85	17.5	16	53

Table 4. Tail impression and digit drag marks parameters. dist m-p: distance pes-manus (mm), FLp/FLm: pes length/manus length (mm), BL: body length (mm). BL/FL: body length/pes length, SL/FL: stride length/pes length, SL/BL: stride length/body length, bsl:tail baseline (mm), mdl: tail midline (mm), WL: wave length (mm), amp: amplitude (mm), TW: tail width (mm).

Specimen	dist m-p	FLp/FLm	sole/palm	BL	BL/FL	SL/FL	SL/BL	bsl	mdl	WL	amp	TW
GONF-A-04	39	1.45	1.37	50	1.78	4.29	2.4	156	160	90	2.7	4-5.5
GONF G 20	21.3	1.75	4.4	184	3.45	11.6 ?	1.9					
GONF G21	19.4	1.25	1.19	141.2	3,18	3.9	1.1	273.5	300		1	8-9
GONF-A-11	20	1	0.8	175	2,86	2.5	0.74	222	255	123.5	52	10

905 **Table 5.** Parameters of the manus and pes of *Captorhinus aguti* and comparisons with the
906 avergage ratios of manus and pes tracks.

Captorhinus aguti	pes	manus	ratio	*C. aguti*	Track averages
Length	50	42.5	pes/manus length	1.18	1.36
Width	55	50	pes length/width	0.9	0.98
digit I/IV	0.5	0.43	manus length/width	0.85	0.9
digit II/IV	0.63	0.71	metatarse/metacarpus	1.65	1.94
digit III/IV	0.81	0.93	length		
digit V/IV	0.63	0.57			
digit IV/length	0.9	0.82			
BL/FL	3,7				

907
908
909
910

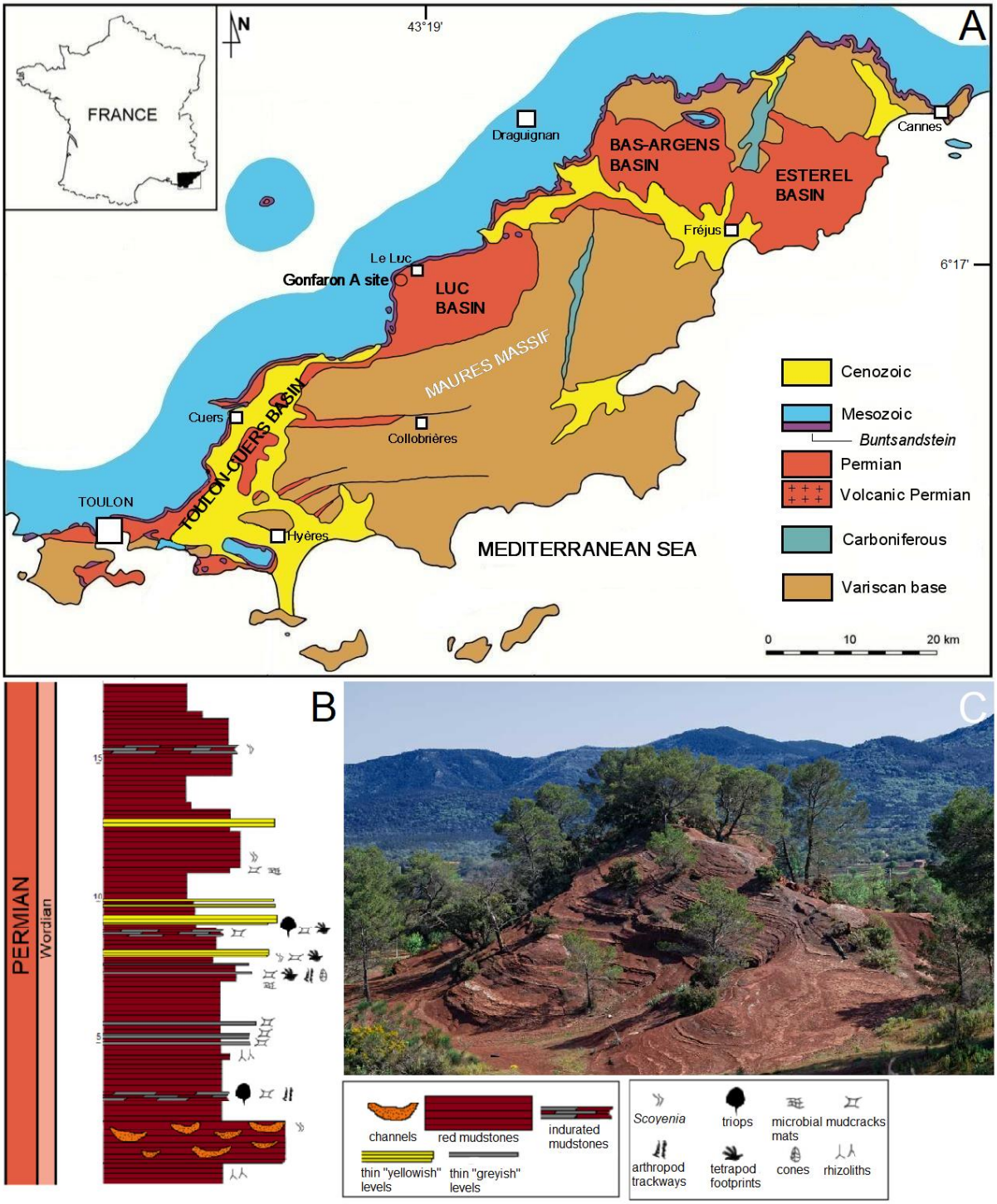

Figure 1 | A. Map of the Permian basins of Provence (after Durand, 2011, modified) with position of the study area and Gonfaron A site with position of footprints levels. B. Stratigraphic log of the Gonfaron A site. C. Photograph of the Gonfaron A site (Romain Garrouste, MNHN).

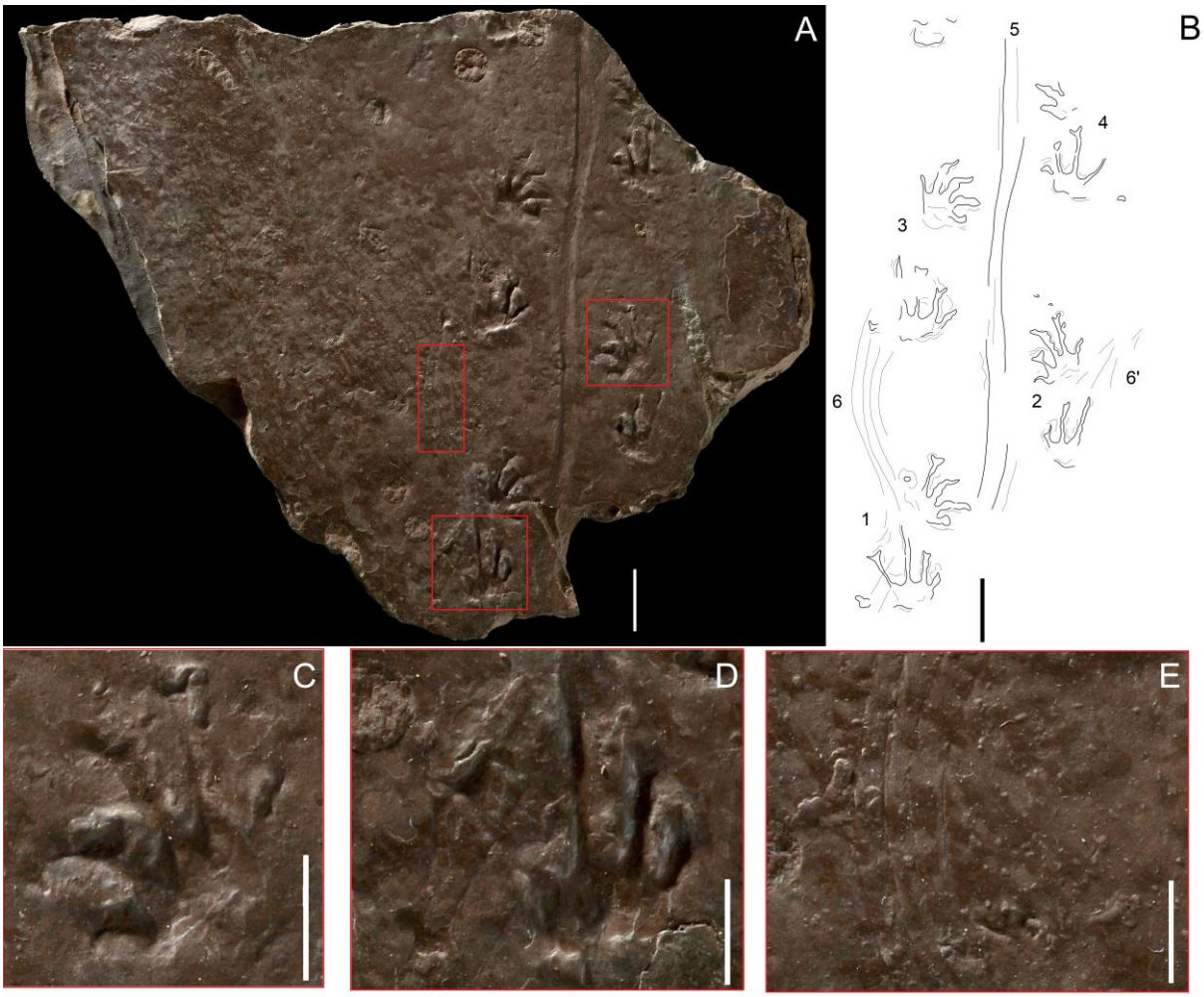

Figure 2 | A. Photograph of *Hyloidichnus* trackways GONF-A-04 with digit drag traces and tail impression. B. Interpretative drawing with Nr. 1 to 4: pes-manus couples, Nr. 5: tail impression, Nr. 6 and 6': digit drag traces. C. Photograph of best preserved right manus imprint. D. Photograph of best preserved left pes imprint. D. Photograph showing details of digit drag traces. Scale bars: 20 mm (A, B), 10 mm (C–E). Photographs by Philippe Loubry, CNRS Paris.

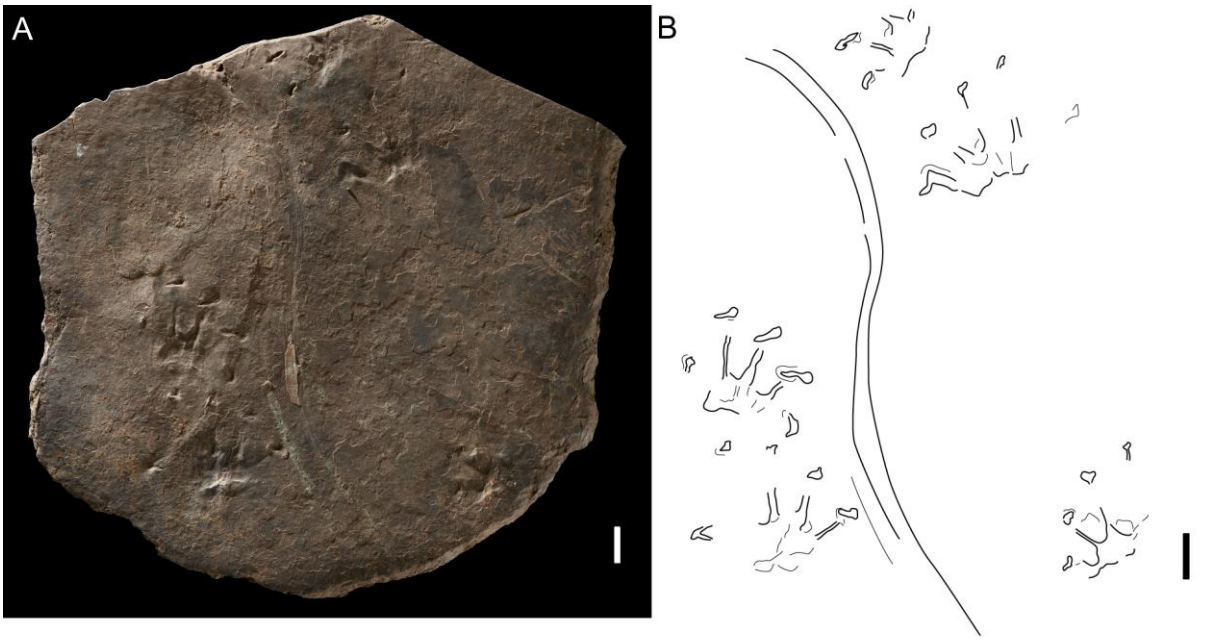

Figure 3 | A. Photograph of *Hyloidichnus* incomplete step cycle GONF-A-11 with sinuous tail impression, concave epirelief. B. Interpretive drawing. Scale bar: 20 mm. Photograph by Phillipe Loubry, CNRS Paris.

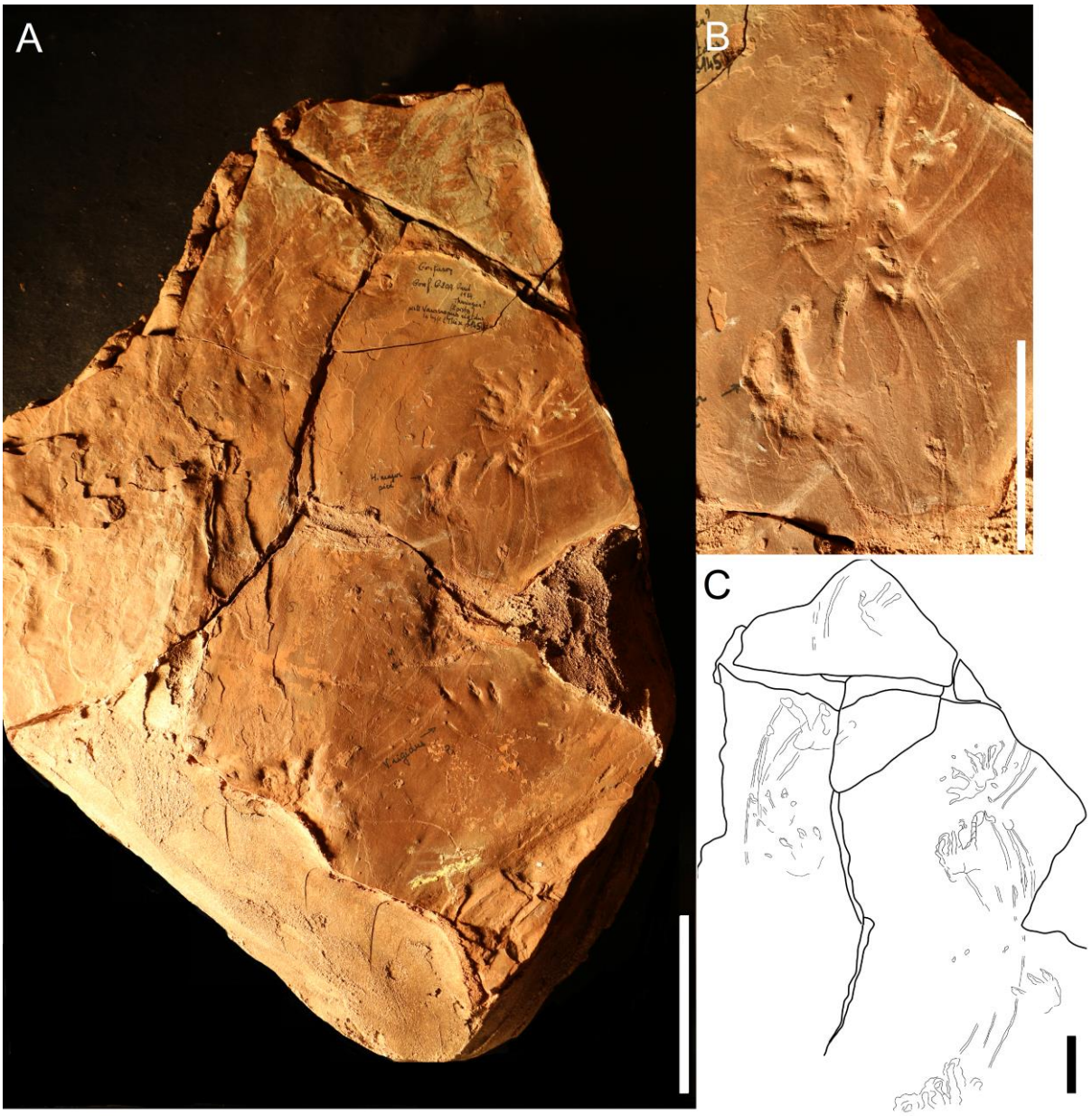

928

929 **Figure 4 |** A. Photograph of *Hyloidichnus* incomplete step cycle GONF-G20 with digit drag
930 marks, convex hyporelief. Note the holotype trackway of *Varanopus rigidus* on the same
931 surface. B. Close-up of left pes-manus couple and digit drag traces. C. Interpretive drawing.
932 Scale bars: 50 mm (A), 40 mm (B, C). Photograph by Lorenzo Marchetti, MB.

933

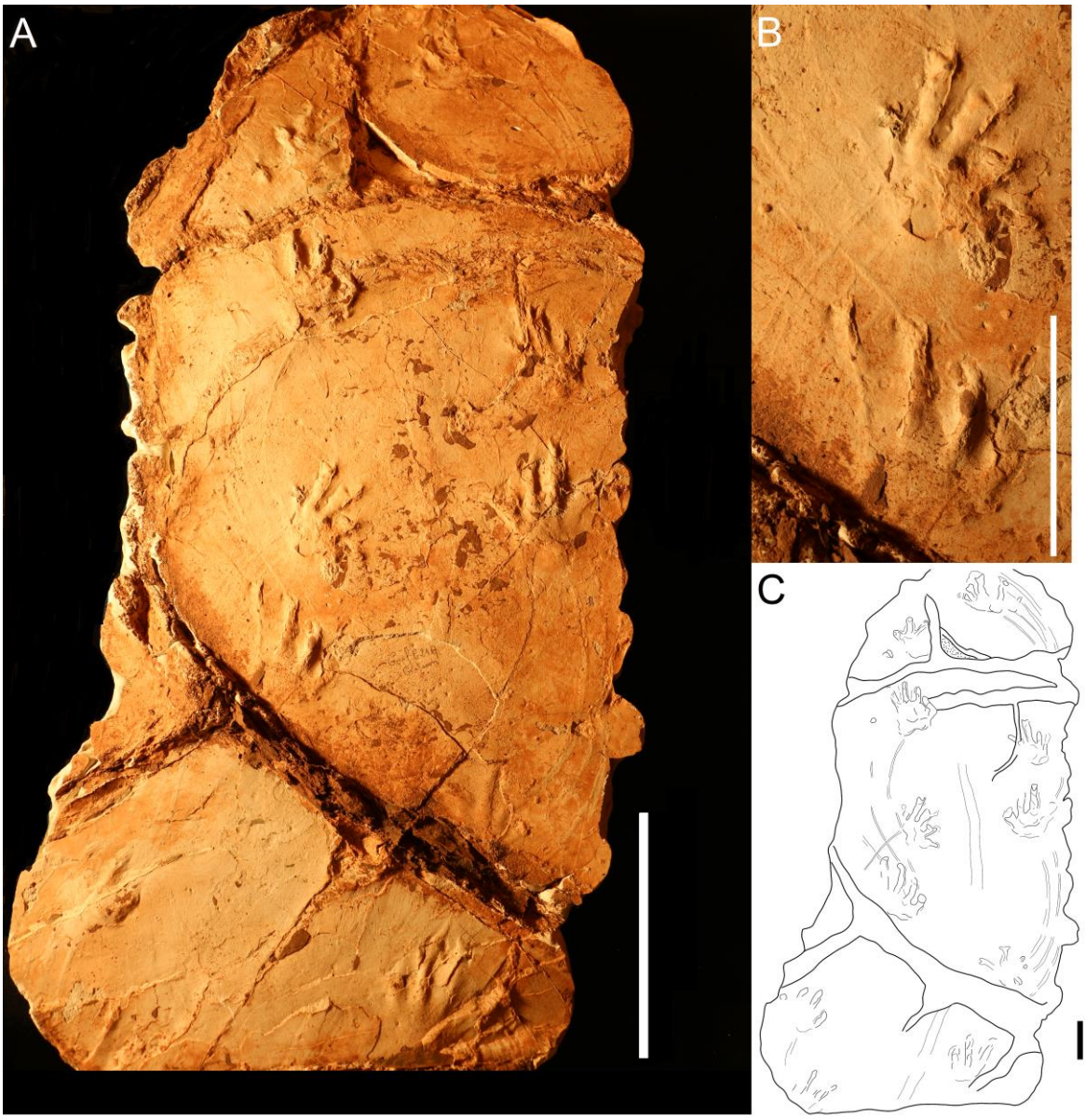

Figure 5 | A. Photograph of *Hyloidichnus* trackway with digit drag traces GONF-G21 with straight and shallow tail impression, convex hyporelief, artificial cast. B. Close up on best preserved right pes-manus couple. C. Interpretive drawing. Scale bars: 10 cm (A), 50 mm (B), 30 mm (C). Photograph by Lorenzo Marchetti, MB.

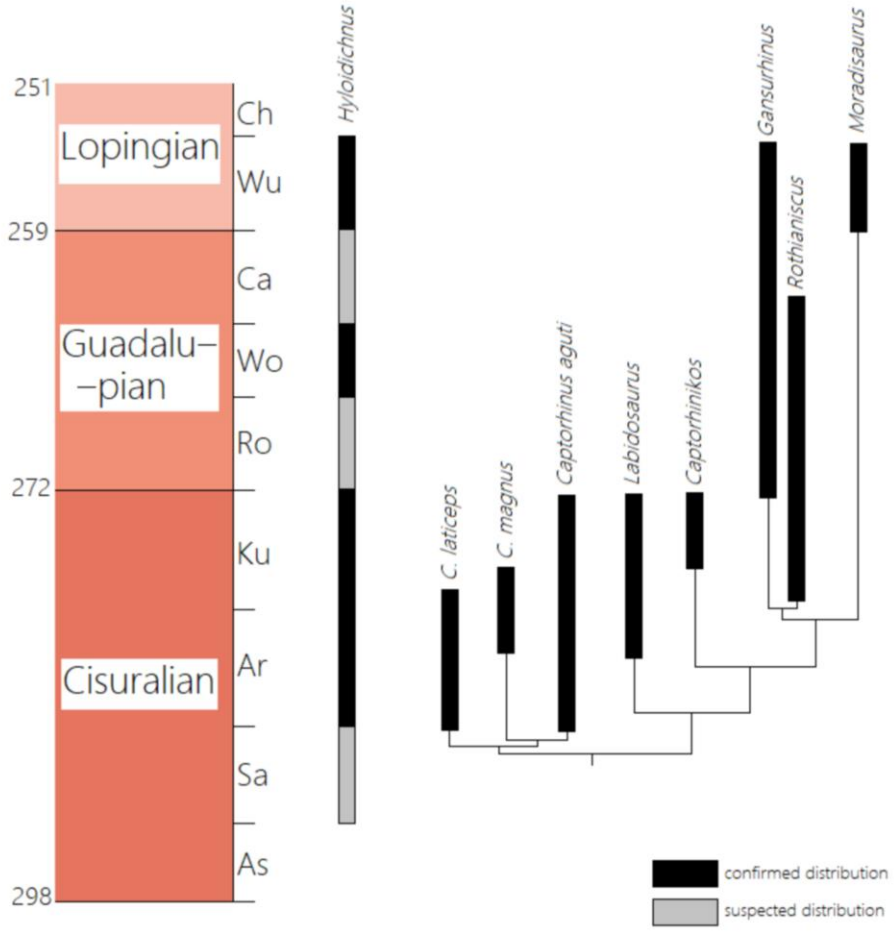

940

941 **Figure 6 |** Stratigraphic distribution of *Hyloidichnus* trackways compared with the consensual
942 stratocladogram of the captorhinomorphs (compiled from The Paleobiology Database
943 https://paleobiodb.org; Modesto and Smith, 2001; Modesto et al., 2019; Voigt and Lucas 2018).

944

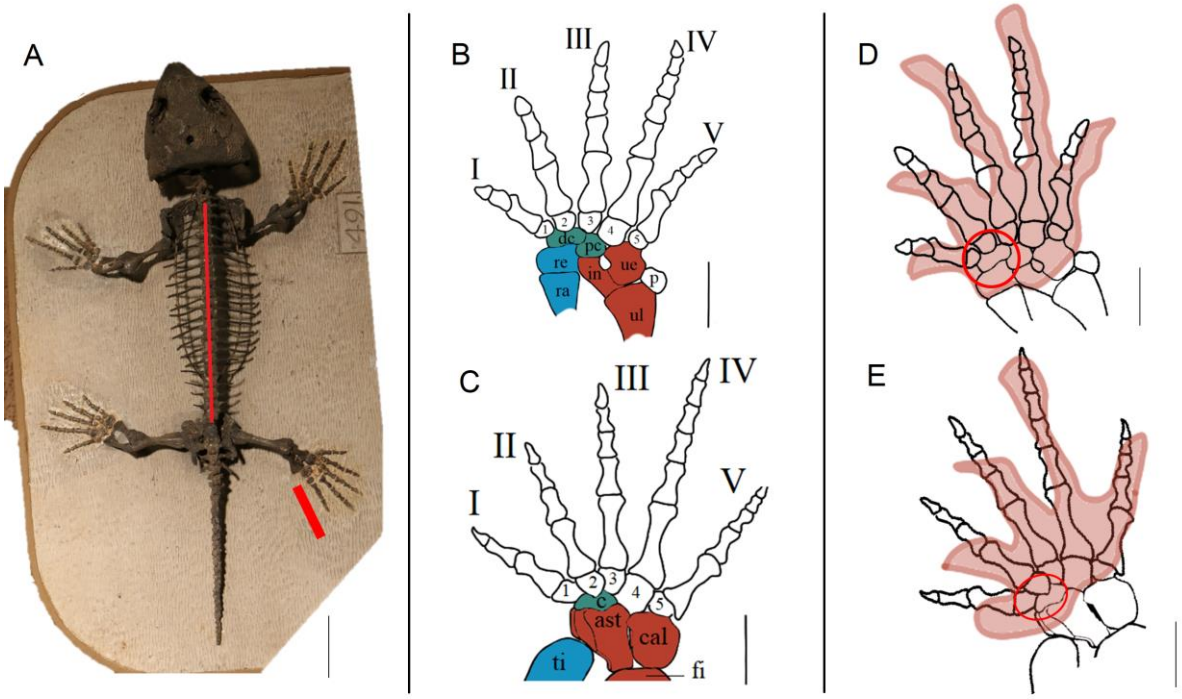

945

946 **Figure 7 |** A. Photograph of skeletal reconstitution of *Captorhinus aguti* (Field Museum of
947 Chicago), the red lines indicate the pes length and the glenoacetabular distance, scale bar: 50
948 mm. B. Anatomy of the manus redrawn after Holmes (1977). ul: ulna, ue: ulnare, in:
949 intermedium, ra: radius, re: radiulare, pc: proximal centrale, dc: distal centrale, 1-5: distal
950 carpals, scale: 10 mm. C. Anatomy of the pes redrawn after Holmes (2003). ti: tibia, fi: fibula,
951 cal : calcaneus, ast: astragalus, c: centrale, 1-5: distal tarsals, scale bar: 10 mm. D. Superposition
952 of the best preserved manus track of specimen GONF-A-04 (in orange) with the skeletal
953 reconstruction of the manus redrawn after Holmes (1977); the red circle indicates the zone with
954 most power flexion during the locomotor cycle, scale bar: 10 mm. E. Superposition of the best
955 preserved pes track of GONF-A-04 (in orange) with the skeletal reconstruction of the pes
956 redrawn after Holmes (2003); the red circle indicates the zone with most power flexion during
957 the locomotor cycle, scale bar: 10 mm. Photograph in A by Lorenzo Marchetti, MB.

958

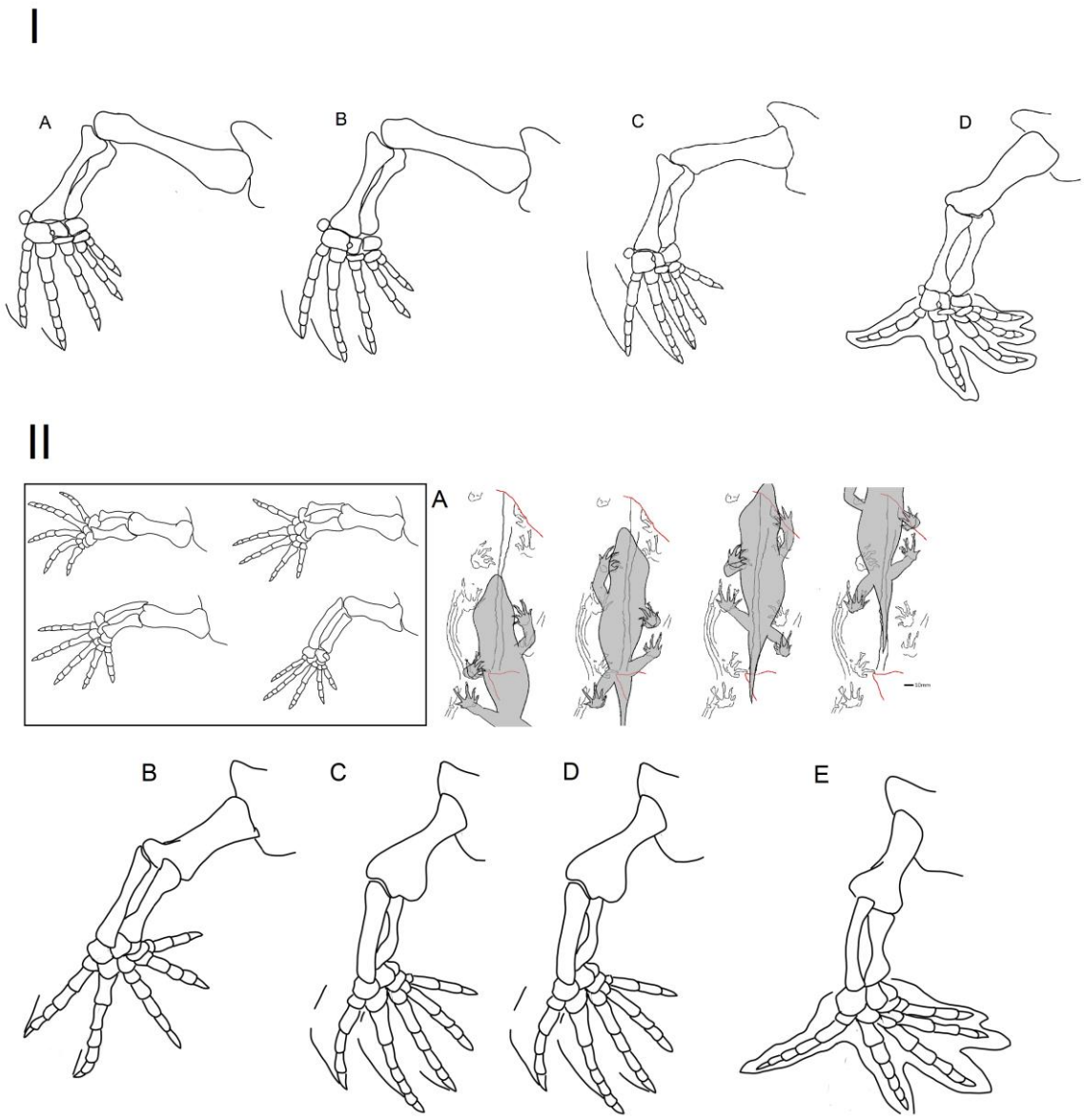

Figure 8 | I. Swing phase of the manus. A. Beginning. B. Early. C. Midstride. D. End. II. Swing phase of the pes. In the square: re-orientation phase between the end of the stance phase and the beginning of the swing phase. A. Reconstruction of captorhinomorph locomotion based on GONF-A-04 trackway. B. Beginning. C. Early. D. Mistride. E. End.

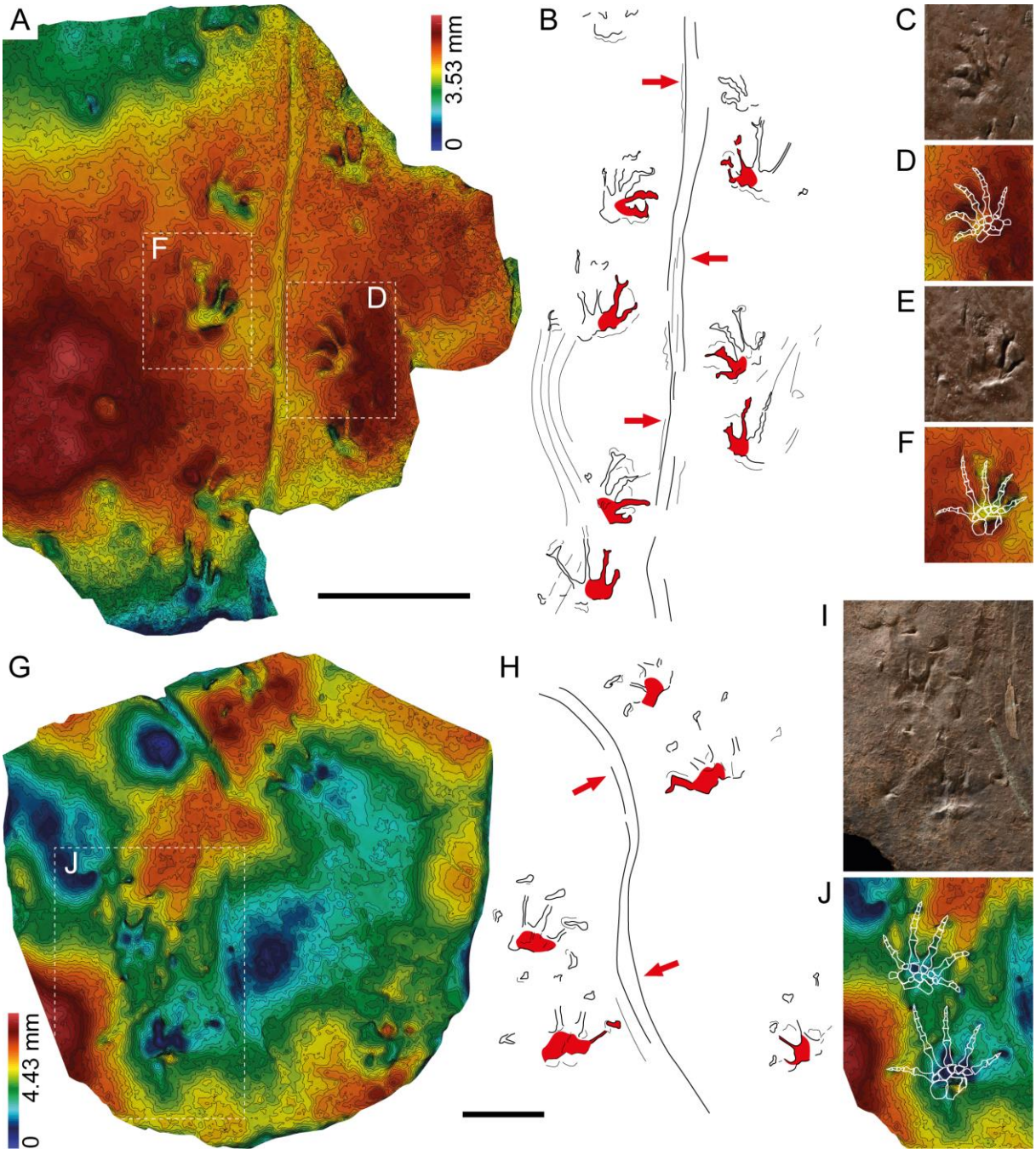

Figure 9 | A. 3D model in false-colour depth and with contours of GONF-A-04. B. Interpretive drawings. C. Photograph of the best preserved right manus track. D. 3D model of the track in C with superimposition of *Captorhinus* manus skeleton. E. Photograph of the best-preserved left pes. F. 3D model of the track in E with superimposition of *Captorhinus* pes skeleton. G. 3D model of GONF-A-11. H. Interpretive drawing. I. Photograph of the left pes-manus couple. J. 3D model of the track in I with superimposition of *Captorhinus* autopodians skeletons. The red zones represent the most deeply impressed part of the imprints. The arrows point to the steepest parts of the tail impressions. *Captorhinus* skeletons after Holmes (2003), modified. Scale bars: 50 mm.

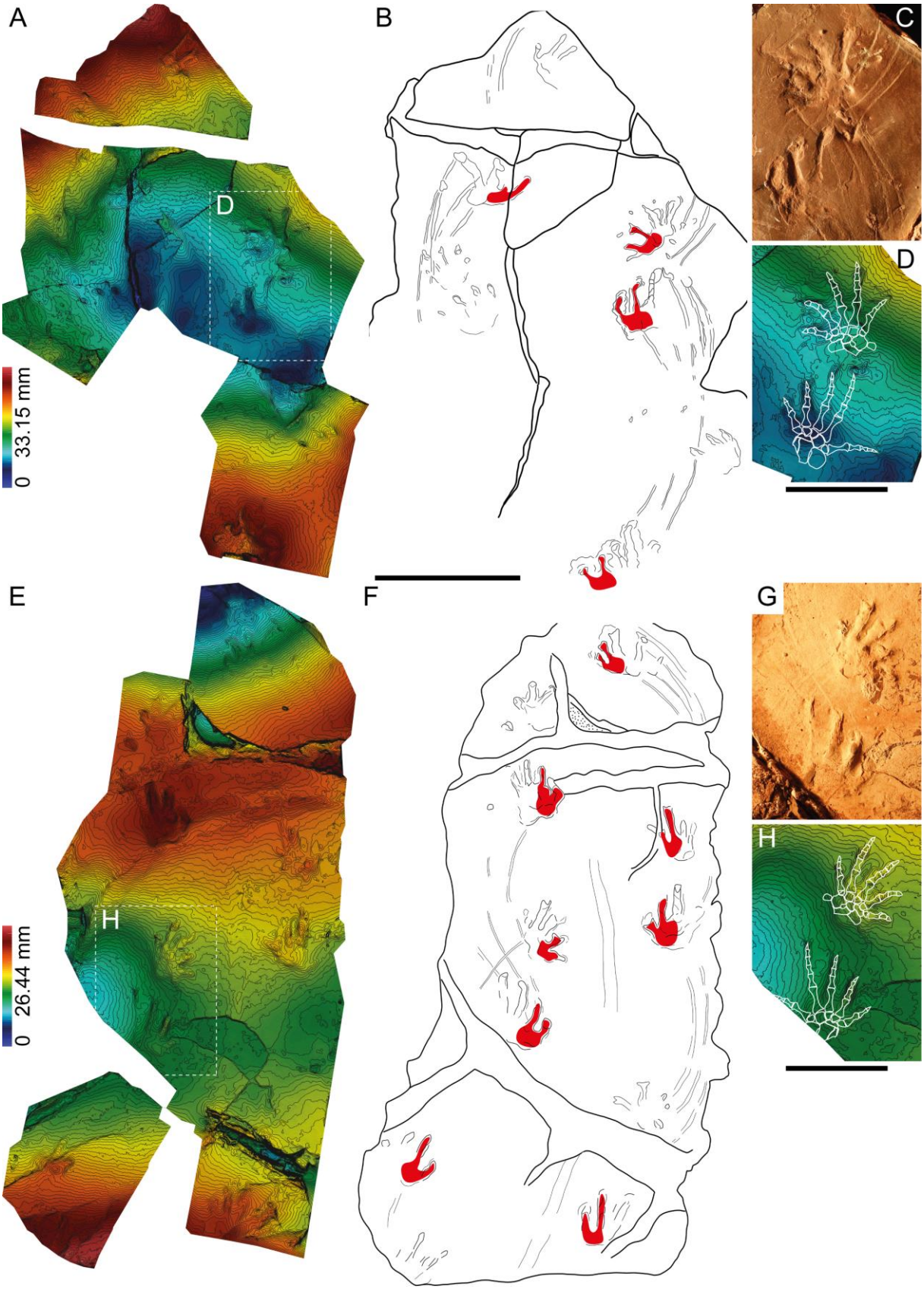

Figure 10 | A. 3D model in false-colour depth and with contours of GONF-G20. B. Interpretive drawing. C. Photograph of the best-preserved left pes-manus couple. D. 3D model of tracks in C with superimposition of *Captorhinus* autopodial skeletons. E. 3D model of GONF-G21. F.

Interpretive drawing. G. Photograph of the best-preserved right pes-manus couple. H. 3D model of the tracks in G with superimposition of *Captorhinus* autopodial skeletons. The red zones represent the most deeply impressed part of the imprints. *Captorhinus* skeletons after Holmes (2003), modified. Scale bars: 10 cm (A, B, E, F), 50 mm (C, D, G, H).